High resolution profiling of RNA synthesis and decay

Caroline C. Friedel[1,2], Lars Dölken[3], Ralf Zimmer[2]

1 Institut für Pharmazie und molekulare Biotechnologie, Universität Heidelberg, Heidelberg
2 Institut für Informatik, Ludwig-Maximilians-Universität München, München
3 Max von Pettenkofer-Institute, Ludwig-Maximilians-Universität München, München

RNA levels in a cell are regulated by RNA synthesis and decay. State-of-the-art gene expression profiling typically only allows measurements of total transcript abundance. It cannot distinguish whether changes in total mRNA are due to alterations in de novo transcription or in decay. Recently (Dölken, et al., 2008; Friedel and Dölken, 2009), we presented a novel approach for measuring both RNA synthesis and decay by labeling nascent RNA (RNA tagging) and separating total cellular RNA into nascent and unlabeled pre-existing RNA. Both RNA fractions together with the total cellular RNA are directly compatible with microarray analysis (Dölken, et al., 2008; Friedel and Dölken, 2009) and RNA-seq (Rabani, et al., 2011; Schwanhäusser, et al., 2011).

We believe that our work will be interesting and important for the audience of GCB for the following reasons:

First, by measuring nascent RNA, the temporal order and kinetics of transcriptional regulation following a stimulus can by analyzed at the time scale of minutes. This avoids a time lag until total mRNA changes can be detected. Thus, both fast and transient primary effects and slow and long-term secondary effects can be identified in a single experiment.

Second, measurements of nascent, pre-existing and total RNA allow an intuitive normalization of microarray experiments by simple linear regression analysis and a quality control to identify unreliable measurements.

Third, transcript half-lives can be determined with superior accuracy and without having to interfere with the transcriptional machinery. This provides new insights into gene regulation, in particular the regulation of protein complexes, and is important for quantitative systems biology modelling (Friedel, et al., 2009). We think that this work will influence the way gene expression profiling experiments will be performed in the future and, thus, this presentation will attract both experimental biologists and bioinformaticians studying the control of gene regulation.

References:

Dölken, L., Ruzsics, Z., Rädle, B., Friedel, C.C., Zimmer, R., Mages, J., Hoffmann, R., Dickinson, P., Forster, T., Ghazal, P. and Koszinowski, U.H. (2008) High-resolution gene expression profiling for simultaneous kinetic parameter analysis of RNA synthesis and decay, *RNA*, **14**, 1959-1972.
Friedel, C.C. and Dölken, L. (2009) Metabolic tagging and purification of nascent RNA: Implications for transcriptomics, *Molecular BioSystems*, **5**, 1271-1278.
Friedel, C.C., Dölken, L., Ruzsics, Z., Koszinowski, U.H. and Zimmer, R. (2009) Conserved principles of mammalian transcriptional regulation revealed by RNA half-life, *Nucleic acids research*, **37**, e115.
Rabani, M., Levin, J.Z., Fan, L., Adiconis, X., Raychowdhury, R., Garber, M., Gnirke, A., Nusbaum, C., Hacohen, N., Friedman, N., Amit, I. and Regev, A. (2011) Metabolic labeling of RNA uncovers principles of RNA production and degradation dynamics in mammalian cells, *Nat Biotechnol*, **29**, 436-442.
Schwanhäusser, B., Busse, D., Li, N., Dittmar, G., Schuchhardt, J., Wolf, J., Chen, W. and Selbach, M. (2011) Global quantification of mammalian gene expression control, *Nature*, **473**, 337-342.

High-resolution gene expression profiling for simultaneous kinetic parameter analysis of RNA synthesis and decay

LARS DÖLKEN,[1] ZSOLT RUZSICS,[1] BERND RÄDLE,[1] CAROLINE C. FRIEDEL,[2] RALF ZIMMER,[2] JÖRG MAGES,[3] REINHARD HOFFMANN,[3] PAUL DICKINSON,[4] THORSTEN FORSTER,[4] PETER GHAZAL,[4] and ULRICH H. KOSZINOWSKI[1]

[1]Max von Pettenkofer-Institute, Ludwig Maximilians-University Munich, Munich 80337, Germany
[2]Institute for Informatics, Ludwig Maximilians-University Munich, Munich 80333, Germany
[3]Institute of Medical Microbiology, Technical University Munich, Munich 81675, Germany
[4]Division of Pathway Medicine and Centre for Systems Biology at Edinburgh, The University of Edinburgh, Edinburgh, Scotland EH16 4SB, United Kingdom

ABSTRACT

RNA levels in a cell are determined by the relative rates of RNA synthesis and decay. State-of-the-art transcriptional analyses only employ total cellular RNA. Therefore, changes in RNA levels cannot be attributed to RNA synthesis or decay, and temporal resolution is poor. Recently, it was reported that newly transcribed RNA can be biosynthetically labeled for 1–2 h using thiolated nucleosides, purified from total cellular RNA and subjected to microarray analysis. However, in order to study signaling events at molecular level, analysis of changes occurring within minutes is required. We developed an improved approach to separate total cellular RNA into newly transcribed and preexisting RNA following 10–15 min of metabolic labeling. Employing new computational tools for array normalization and half-life determination we simultaneously study short-term RNA synthesis and decay as well as their impact on cellular transcript levels. As an example we studied the response of fibroblasts to type I and II interferons (IFN). Analysis of RNA transcribed within 15–30 min at different times during the first three hours of interferon-receptor activation resulted in a >10-fold increase in microarray sensitivity and provided a comprehensive profile of the kinetics of IFN-mediated changes in gene expression. We identify a previously undisclosed highly connected network of short-lived transcripts selectively down-regulated by IFNγ in between 30 and 60 min after IFN treatment showing strong associations with cell cycle and apoptosis, indicating novel mechanisms by which IFNγ affects these pathways.

Keywords: microarray; biosynthetic labeling; half-life; 4-thiouridine; interferon

INTRODUCTION

Multiple regulatory processes govern the flow of genetic information from DNA to protein. Stimulated cells alter transcription rates of individual genes within minutes (Liu et al. 2007). Characteristic and differential mRNA turnover rates either contribute to rapid changes in cellular gene expression profiles or rigidly maintain constant transcript levels. Thus, mRNA levels of genes at a given time are the result of an intensively regulated balance between de novo transcription and mRNA decay (Guhaniyogi and Brewer 2001; Fan et al. 2002; Jing et al. 2005).

Reprint requests to: Lars Dölken, Max von Pettenkofer-Institut Pettenkoferstraße 9a, D-80336 München, Germany; e-mail: doelken@mvp.uni-muenchen.de; fax: +49-89-5160-5292.

Article published online ahead of print. Article and publication date are at http://www.rnajournal.org/cgi/doi/10.1261/rna.1136108.

Standard microarray analyses on total cellular RNA (total RNA) provide a measure of mRNA abundance but cannot discriminate whether changes are due to alterations in RNA synthesis or decay. Numerous attempts have been undertaken to circumvent this problem. De novo transcription and its contribution to steady-state mRNA levels were determined using nuclear transcription run-on assays (Hirayoshi and Lis 1999; Fan et al. 2002; Garcia-Martinez et al. 2004). However, these assays are not readily compatible with standard microarray formats. Decay rates have been determined by blocking transcription, e.g., using actinomycin-D (act-D), assuming mRNA decay to continue at its normal rate (Frevel et al. 2003; Yang et al. 2003; Bernstein et al. 2004; Raghavan and Bohjanen 2004). However, this method is inherently cell invasive and cannot be combined with assays used to measure de novo transcription.

Low temporal resolution for regulatory changes is another major limitation of standard expression profiling

using total RNA. This is particularly true for mammalian cells due to the relatively long half-life of their mRNAs. While the median mRNA half-life ($t_{½m}$) in prokaryotic cells is in the range of 20–30 min (Bernstein et al. 2002), $t_{½m}$ in human cells was reported to be 600 min (Yang et al. 2003). Hence, even hours after a >100-fold transient down-regulation in transcription rate, this is hardly detectable in total RNA without concordant changes in mRNA decay. In addition, for the majority of transcripts a 10-fold up-regulation in transcription rate requires >2 h to result in a twofold increase in abundance. Therefore, primary changes cannot be differentiated from subsequent events by assays measuring transcript abundance only.

It has been known for 30 years that thiol-group containing nucleosides such as 4-thiouridine (4sU) can be introduced into nucleoside salvage pathways in eukaryotic cells and allow nondisruptive metabolic labeling of newly transcribed RNA (Melvin et al. 1978). These can be used to separate newly transcribed RNA from total RNA using mercury affinity chromatography (Melvin et al. 1978; Woodford et al. 1988; Ussuf et al. 1995; Kenzelmann et al. 2007) or thiol-specific biotinylation and subsequent purification on streptavidin-coated magnetic beads (Cleary et al. 2005) as eukaryotic mRNAs normally do not contain thiol-groups. Here we report on an integrated, improved approach in which the advantages of direct incorporation of 4sU are combined with thiol-specific biotinylation and simple magnetic separation of total RNA into newly transcribed RNA and preexisting unlabeled RNA. This allows microarray analysis on all three obtained RNA subsets in parallel. Thus, for the first time, changes in RNA synthesis and decay as well as their impact on cellular transcript levels can be analyzed in a single experimental setting.

Theoretically, short-term biosynthetic labeling for 15–30 min at different times during cytokine treatment should allow differentiation of the temporal order and kinetics of changes in gene expression at molecular level. We demonstrate this by analyzing the cellular response to type I and II interferons (IFN). IFNs are an intensively studied family of multifunctional cytokines known to dramatically alter transcription rates of hundreds of transcripts (for review, see Platanias 2005). They play an essential role in innate immunity in response to viral, bacterial, and parasitic pathogens (Stetson and Medzhitov 2006). In addition, they exert important anti-proliferative as well as immune modulatory properties (Boxel-Dezaire et al. 2006).

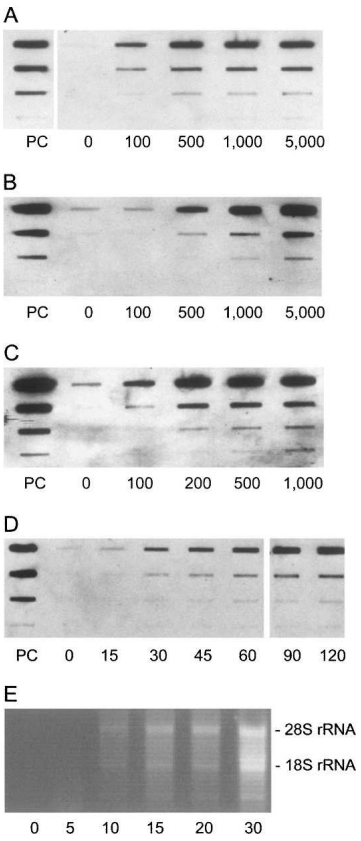

FIGURE 1. Detection and quantification of 4sU incorporation into RNA. 4sU is quantitatively incorporated into newly transcribed RNA by a broad range of cell lines of human and murine origin. Dot blot analyses of thiol-mediated biotinylation of RNA derived from (*A*) murine NIH-3T3 fibroblasts, (*B*) SVEC 4-10 endothelial cells, and (*C*) DG75 human B-cells exposed to 100 μM to 5 mM 4sU for 1 h are shown as examples. Nonlabeled RNA samples (0) were used as controls. All RNA samples were spotted in 10-fold dilutions (*top* to *bottom*: 1 μg down to 1 ng). A 5′-biotinylated DNA oligo of 81 nt (PC) was used in 10-fold dilutions (100 ng down to 0.1 ng) to quantify biotin-labeling. (*D*) Kinetics of 4sU incorporation into cellular RNA were analyzed. NIH-3T3 cells were cultured in the presence of 1 mM 4sU for 0, 15, 30, 45, 60, 90, and 120 min. Dot blot analyses of biotinylated RNA samples are shown as for *A*–*C*. (*E*) Newly transcribed RNA was labeled in NIH-3T3 cells using 500 μM 4sU for 0, 5, 10, 15, 20, and 30 min. Following isolation of total cellular RNA and thiol-specific biotinylation, newly transcribed RNA was purified from 100 μg biotinylated total RNA. Half of the purified RNA was separated on an ethidium bromide-stained agarose gel under nondenaturating conditions.

RESULTS

Separation of total cellular RNA into newly transcribed and preexisting RNA

Metabolic labeling of newly transcribed RNA with 4sU has minimal adverse effects on gene expression, RNA decay, protein stability, and cell viability (Melvin et al. 1978; Woodford et al. 1988; Ussuf et al. 1995; Kenzelmann et al. 2007). We compared the global transcriptional profile of three biological replicates of NIH-3T3 cells exposed to 200 μM 4sU for one hour with nontreated cells. No significant differential expression (more than twofold and $P < 0.05$) attributable to 4sU treatment was detected (see Supplemental Fig. 1). We analyzed 4sU incorporation into newly transcribed RNA by culturing various cell types in the presence of 100 μM to 5 mM 4sU for one hour. Following isolation of total cellular RNA and thiol-specific biotinylation,

TABLE 1. Comparison of RNA ratios and half-lives obtained by RNA labeling and by blocking transcription using act-D

	Newly transcribed/total RNA		1 h act-D		2 h act-D	
Gene title	Ratio (%)	$t_{1/2}$ (h)	Ratio (%)	$t_{1/2}$ (h)	Ratio (%)	$t_{1/2}$ (h)
Dual specificity phosphatase 5	94.4	0.2	11.5	0.3	2.2	0.4
Dual specificity phosphatase 6	93.5	0.2	8.0	0.3	3.0	0.4
Jun oncogene	74.6	0.5	22.4	0.5	6.6	0.5
Fos oncogene	54.1	0.8	83.8	3.9	13.2	0.7
Suppressor of cytokine signaling 3	67.6	0.6	5.2	0.2	5.9	0.5
Suppressor of cytokine signaling 5	55.4	0.8	37.0	0.7	35.2	1.3
E2F transcription factor 3	38.8	1.3	56.1	1.2	12.4	0.7
E2F transcription factor 7	36.5	1.4	59.6	1.3	21.5	0.9
Cyclin T2	25.0	2.2	48.4	1.0	23.4	1.0
Cyclin L2	24.5	2.3	113.9	NC	83.3	7.6
Lamin B1	8.5	7.2	95.6	15.3	60.1	2.7
Myosin IB	8.4	7.2	105.0	NC	76.4	5.2
Proteasome (prosome, macropain) subunit, beta type 6	6.2	10.0	107.9	NC	84.3	8.1
Proteasome (prosome, macropain) subunit, beta type 4	6.1	10.1	115.5	NC	78.9	5.8
Proteasome (prosome, macropain) subunit, alpha type 5	5.9	10.5	81.4	3.4	67.5	3.5
NADH dehydrogenase (ubiquinone) Fe-S protein 1	4.7	13.1	96.2	18.0	74.6	4.7
NADH dehydrogenase (ubiquinone) Fe-S protein 8	4.4	14.0	77.3	2.7	87.1	10.0
NADH dehydrogenase (ubiquinone) Fe-S protein 3	4.2	14.7	99.0	67.1	77.0	5.3
ATP synthase, H+ transporting, mitochondrial F1 complex, epsilon subunit	2.0	30.8	84.1	4.0	81.6	6.8
ATP synthase, H+ transporting, mitochondrial F0 complex, subunit d	1.9	33.5	95.1	13.9	82.3	7.1
Catalase	1.2	51.7	92.0	8.3	89.2	12.1
Procollagen, type IV, alpha 5	1.2	53.2	72.3	2.1	83.5	7.7

In NIH-3T3 cells newly transcribed RNA was labeled for 60 min using 200 μM 4sU. Total cellular RNA was isolated and newly transcribed RNA was purified. In a second experiment carried out in parallel, RNA synthesis was blocked for 1 and 2 h using act-D. Microarray analysis was performed on three replicates of each RNA subset. Array data for newly transcribed RNA and total RNA were normalized by adjusting the median newly transcribed RNA/total RNA ratio to the ratio calculated for the median mRNA half-life we determined for NIH-3T3 cells (295 min). The same was done for the act-D-based ratios and half-lives were calculated as described (Yang et al. 2003). Examples of short-, medium-, and long-lived genes with similar function are shown. For ratios >100% no half-life can be calculated (NC).

4sU-labeled RNA was specifically detected and quantified by dot blot assay. We found 4sU to be efficiently incorporated into RNA by a broad range of cell types of human and murine origin including fibroblasts, endothelial cells, and B-cells (Fig. 1A–C) as well as dendritic cells, macrophages, and T-cells (data not shown). Labeled RNA was detectable by dot blot analysis after 15 min of labeling (Fig. 1D).

In cells expressing *Toxoplasma gondii* uracil-phosphoribosyltransferase (UPRT) newly transcribed RNA can be metabolically labeled using 4-thiouracil (4tU) (Cleary et al. 2005). In this report newly transcribed RNA was isolated by thiol-specific biotinylation followed by affinity purification on streptavidin-coated magnetic beads. We adapted this approach to 4sU labeling, which does not require UPRT expression. We established an improved, column-based protocol for magnetic separation of total RNA into newly transcribed RNA and preexisting RNA (for details, see Materials and Methods). Employing this approach, high-molecular-weight newly transcribed RNA could be detected by agarose gel electrophoresis after as little as 10 min of labeling (Fig. 1E). After one hour of labeling newly transcribed RNA accounted for 3%–6% of total RNA depending on the cell type under study (data not shown). The efficiency of separation was validated by combining 4sU and ^{3}H-cytidine to label newly transcribed RNA for 15, 30, and 60 min. After thiol-specific biotinylation up to 90% of ^{3}H-cytidine-labeled RNA copurified with the newly transcribed RNA fraction (see Supplemental Fig. 2A–D). When ^{3}H-labeled, unbiotinylated RNA was subjected to this separation procedure, the first two of a total of six washing steps already contained the bulk of labeled RNA, indicating preparative recovery of both newly transcribed

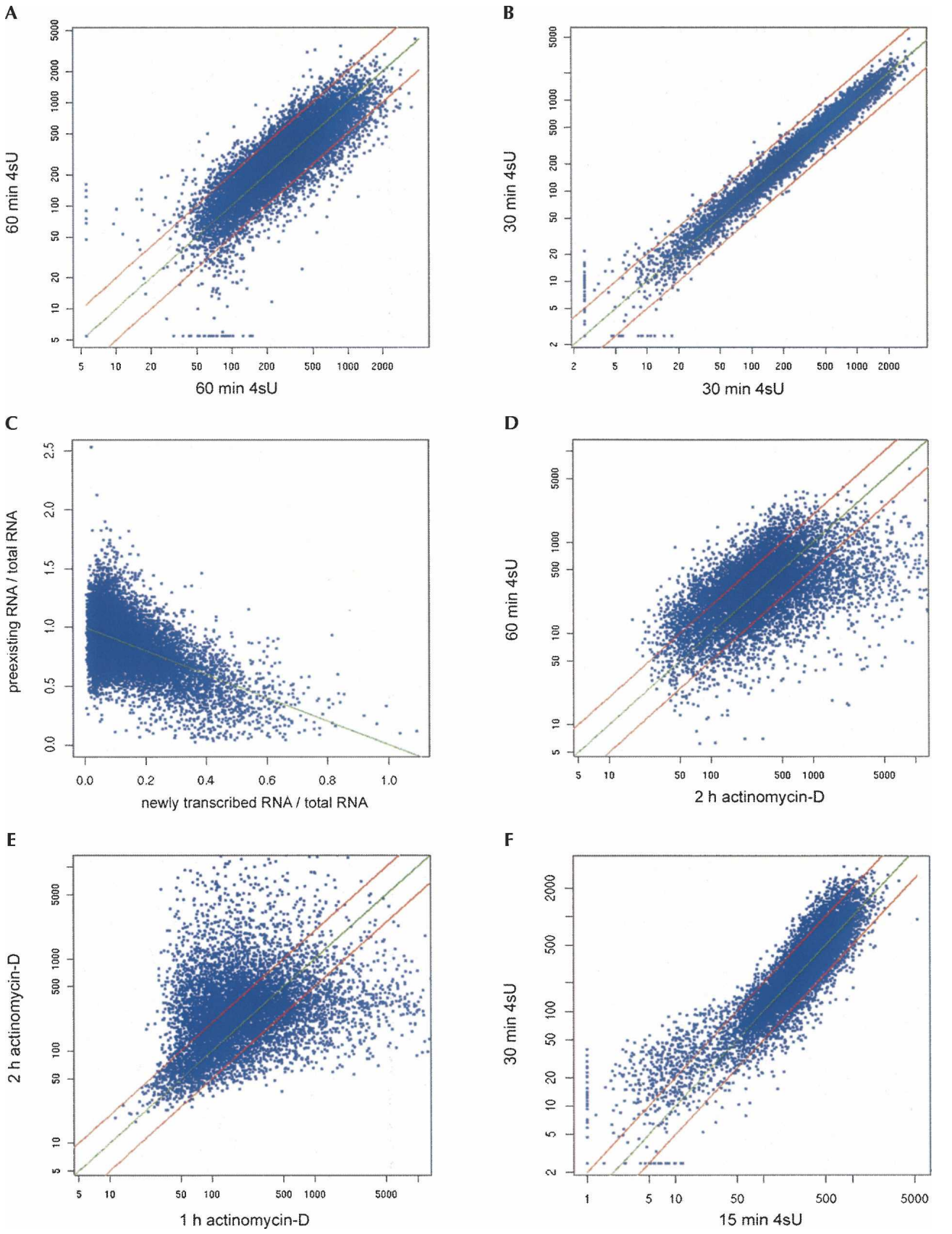

FIGURE 2. (Legend on next page)

RNA and preexisting RNA from total RNA. Thus, both RNA subsets, present in the same isolated RNA sample, can be separated with high purity.

Development of an integrative approach to simultaneously analyze RNA synthesis and decay

For every transcript total RNA levels are constantly subjected to changes in RNA synthesis and decay. So far it was not possible to analyze both parameters in a systemic approach in a single experimental setting. The standard method used to study RNA decay is to block transcription, e.g., using act-D (Frevel et al. 2003; Yang et al. 2003). However, this approach has a number of limitations. First, blocking transcription provokes a cellular stress response. Some important mechanisms that control mRNA stability, e.g., miRNA-mediated control of gene expression (Jing et al. 2005), are released in cells subjected to stress (Bhattacharyya et al. 2006). In addition, some transcripts have been shown to be rapidly stabilized following act-D treatment (Shyu et al. 1989). Second, for the vast majority of mammalian mRNAs, decay rates determined by blocking transcription are based on very small differences in transcript levels. Only in the case of very short-lived transcripts ($t_{1/2}$ < 2 h), RNA levels decrease by >50% upon 2 h of transcriptional blockage. Thus, act-D-based measurements of RNA decay are inherently imprecise for the majority of cellular transcripts.

We developed a novel approach to simultaneously study RNA synthesis and decay for which blocking transcription is not required. Under steady-state conditions, RNA synthesis compensates for RNA decay to maintain stable transcript levels. Therefore, de novo synthesis rates are much higher for short-lived transcripts than for long-lived transcripts. In murine fibroblasts, we found newly transcribed RNA/total RNA ratios to vary from 1% to 2% for long-lived to >95% for very short-lived transcripts (for examples, see Table 1). Based on the newly transcribed RNA/total RNA ratios (R) and the duration of labeling (t_L) precise data on mRNA half-life ($t_{1/2}$) can be calculated according to the following equation: $t_{1/2} = -t_L \times \ln(2) / \ln(1 - R)$ (for details, see Supplemental Methods). Thus, assuming steady-state conditions mRNA synthesis and decay rates can be determined by simply analyzing newly transcribed RNA and total RNA derived from the same RNA sample.

We applied this approach to determine mRNA half-lives for murine fibroblasts. Newly transcribed RNA was labeled in NIH-3T3 cells for 60 and 30 min. After isolation of total cellular RNA newly transcribed RNA was separated from it. Three replicates of both total RNA and newly transcribed RNA were subjected to microarray analysis. Half-life measurements based on newly transcribed RNA/total RNA ratios resulted in precise and reproducible data independent of mRNA half-life ranging from <20 min to >2 d (Fig. 2A,B).

If steady-state conditions are not given there is no equilibrium in between RNA synthesis and decay. Therefore, only RNA synthesis is analyzed using newly transcribed RNA while RNA decay is determined by comparing preexisting RNA obtained after the application of a stimulus, e.g., a cytokine, with total RNA levels prior to it [$t_{1/2} = -t_L \times \ln(2) / \ln(P)$, with P = preexisting RNA/total RNA]. Thereby, the polar effects of act-D treatment on RNA decay are avoided as, instead of blocking RNA synthesis, newly transcribed RNA is physically separated from total RNA.

For act-D-based determination of RNA decay rates, array data from RNA samples obtained after blocking transcription have to be adjusted to data from samples prior to it. This kind of normalization is usually based on the mRNA half-life of a housekeeping gene (e.g., β-actin) independently determined in a separate experiment (Yang et al. 2003). It is a crucial step for comparing data from independent experiments and is also required when RNA half-lives are determined based on newly transcribed RNA/total RNA or preexisting RNA/total RNA ratios. We developed a novel approach to solve this task by statistical means based on the separation of total RNA into newly transcribed and preexisting RNA. For all probe sets the sum

FIGURE 2. (*A*,*B*) Analysis of mRNA half-lives determined based on newly transcribed RNA/total RNA ratios. Newly transcribed RNA was labeled in NIH-3T3 cells for 60 or 30 min. Total cellular RNA was separated into newly transcribed RNA and unlabeled preexisting RNA. For each experiment three biological replicates of each RNA subset were subjected to microarray analysis. For each condition half-lives were determined based on newly transcribed RNA/total RNA ratios obtained from >13,000 probe sets. Scatterplots comparing half-lives (in minutes) obtained by 60 min of labeling in separated experiments (*A*) and by 30 min of labeling within a single experiment (*B*) are shown. Red lines indicate deviations from the regression line (green) by twofold in either direction. (*C*) Normalization of total RNA, newly transcribed RNA, and preexisting RNA microarray data using linear regression analysis. Preexisting RNA/total RNA ratios were plotted against newly transcribed RNA/total RNA ratios. As total RNA is separated into newly transcribed RNA and preexisting RNA, the sum of the two ratios should equal 100% for every transcript. Therefore, a linear correlation exists between the two ratios and linear regression analysis (green line) can be used to determine the parameters required for correct data normalization. Thereby, a median mRNA half-life of 295 min was determined for NIH-3T3 cells. (*D*–*F*) Comparison of mRNA half-lives obtained by RNA labeling and actinomycin-D treatment (act-D). In parallel to the RNA labeling experiments, RNA synthesis was blocked in NIH-3T3 cells for 1 and 2 h using act-D. Microarray analyses were performed on three replicates of each RNA subset. (*D*) Half-lives determined by 2 h act-D treatment and 60 min of labeling correlated reasonably well. (*E*) Half-lives (in minutes) determined by blocking transcription for 1 and 2 h using act-D only correlated well for very short-lived transcripts ($t_{1/2}$ < 2 h) but poor for the remaining transcripts. (*F*) Half-lives (in minutes) obtained by 15 and 30 min of labeling within a single experiment were compared to identify potential effects caused by 4sU labeling. Significant differences were only observed for very short-lived transcripts ($t_{1/2}$ < 50 min).

of the ratios of newly transcribed RNA/total RNA and preexisting RNA/total RNA must equal 100% as total RNA is separated into newly transcribed RNA and preexisting RNA. Due to the linear relation between the two ratios, normalization parameters simply result from linear regression analysis. Thus, normalization is based on thousands of probe sets and does not require data from separate experiments (for details, see Supplemental Methods). To demonstrate this, we labeled RNA in NIH-3T3 cells for one hour and separated newly transcribed RNA from preexisting RNA. Three replicates of each RNA subset were subjected to microarray analysis. Normalization parameters were determined based on linear regression analysis on array data of >13,000 probe sets with "present" calls in all arrays (Fig. 2C). mRNA half-lives were obtained using both the newly transcribed RNA/total RNA as well as preexisting RNA/total RNA ratios. The median mRNA half-life ($t_{1/2m}$) in NIH-3T3 fibroblasts was 295 min. To our knowledge a median mRNA half-life in cells of murine origin has not been described. Once the median mRNA half-life of a given cell type has been determined, array normalization can be achieved by normalizing the median newly transcribed RNA/total RNA ratio to the corresponding ratio predicted for the median mRNA half-life.

In order to validate our new approach we compared mRNA half-lives obtained from NIH-3T3 fibroblasts based on newly transcribed RNA/total RNA ratios with data obtained by the standard method, i.e., by blocking transcription for 1 and 2 h using act-D. Data obtained by 2 h act-D and 60 min of labeling correlated reasonably well (Fig. 2D). In contrast, decay rates obtained by blocking transcription (1 h versus 2 h act-D) only correlated well for transcripts with a half-life of <2 h (Fig. 2E). In order to analyze the effect of time on our new method and show that precise data on mRNA half-life can already be determined after very short labeling, we compared half-lives obtained by 15 and 30 min of labeling. We found half-lives to correlate extremely well (Fig. 2F).

Interestingly, there is deviation from the linear correlation for small values ($t_{1/2}$ < 60 min, <5% of all transcripts) and this was also seen when comparing half-lives obtained by 15 and 60 as well as 30 and 60 min of labeling (see Supplemental Fig. 3A,B). This may in part be attributed to the effects of noise in the newly transcribed RNA/total RNA ratios on the logarithmic function used to calculate $t_{1/2}$. However, due to their rapid decay, their half-lives can also be determined with high precision based on preexisting RNA/total RNA ratios (see Supplemental Methods).

Monitoring interferon-mediated differential gene expression

Numerous studies on both type I and II IFN-mediated gene regulation have provided detailed knowledge of their effects on cellular gene expression (for review, see de Veer et al. 2001). For most IFN-regulated genes changes in transcript levels only start to become detectable after 2–3 h. Thus, primary and secondary events are difficult to differentiate. We applied our method to analyze IFN-mediated gene regulation in order to show the advantages of this type of analysis. In a first experiment NIH-3T3 cells were treated for one hour with either 100 U/mL IFNα, 100 U/mL IFNγ, or Φ, adding 4sU at the same time. Total cellular RNA was isolated from cells and newly transcribed RNA was purified. Three biological replicates of each RNA subset were subjected to microarray analysis. In a second larger experiment short-term 4sU labeling was performed at different time intervals during IFN treatment. Specifically, RNA was labeled during the first 15 and 30 min of IFN receptor activation and for 30 min starting 30, 90, and 150 min thereafter. Microarray analyses were performed for three replicates of newly transcribed RNA labeled from 0 to 30, 30 to 60, and 150 to 180 min and from total RNA following 3 h of IFN treatment. In all experiments the number of probe sets showing significant ($P \leq 0.05$) (more than fourfold) up-regulation or (less than twofold) down-regulation was substantially higher for newly transcribed RNA than for total RNA (Fig. 3A–D). Analysis of newly transcribed RNA (30–60 min) instead of total RNA (1 h) increased sensitivity for detection of up- and down-regulation by more than five- and >10-fold, respectively. Interestingly, down-regulation during the first 60 min was exclusively seen after IFNγ treatment.

For further analysis microarray data from all experiments were combined including only probe sets >2-fold regulated and significant ($P \leq 0.01$) in any of the 12 statistical comparisons (n = 957, corresponding to 562 unique genes; for complete list, see Supplemental Table 1). All transcripts which showed significant regulation by >2-fold during the first hour of IFNα or IFNγ treatment were sorted by their half-life (Fig. 4A–C). The median mRNA half-life of genes up-regulated by IFNγ ($t_{1/2m}$ = 184 min) was significantly shorter than for IFNα ($t_{1/2m}$ = 346 min; $P < 0.0001$). We observed a strong correlation between differential gene expression detectable in total RNA at 1 h and transcript half-life. Similar changes for total RNA and newly transcribed RNA were only detectable for short-lived, up-regulated transcripts. In contrast, analysis of newly transcribed RNA revealed substantial differential expression independent of transcript half-life, thereby explaining the superior sensitivity observed when analyzing newly transcribed RNA.

By quantitative PCR, up-regulation of two major IFN-induced transcription factors, *irf1* (interferon regulatory factor 1) and *socs3* (suppressor of cytokine signaling 3) by eight- and fivefold, respectively, was already detectable in newly transcribed RNA after 15 min of IFNγ treatment (see Supplemental Fig. 4). By microarray analysis of newly transcribed RNA substantial changes in gene expression were detected after 30 min (data for all conditions

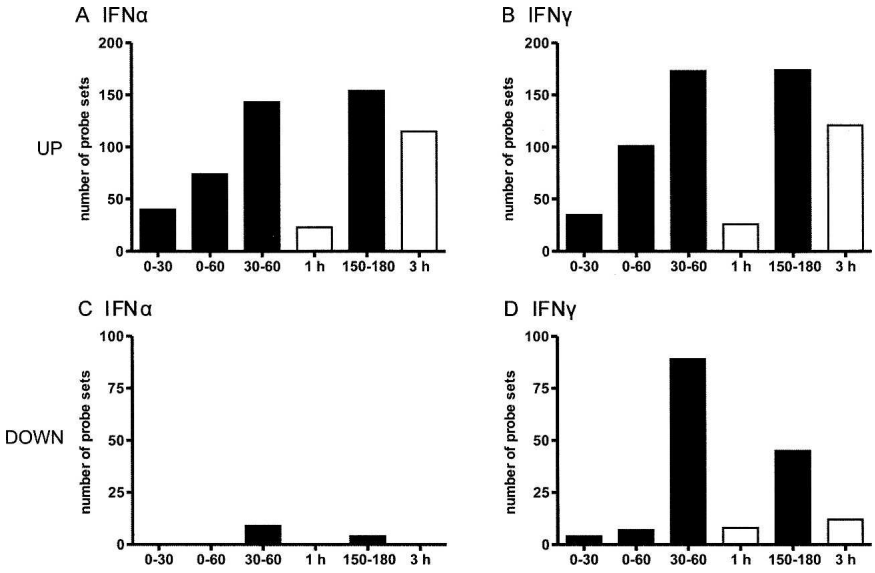

FIGURE 3. Detection of IFN-mediated differential gene expression in newly transcribed RNA and total RNA. NIH-3T3 cells were treated with 100 U/mL of either IFNα or IFNγ or were left untreated. Newly transcribed RNA was labeled by adding 500 μM 4sU (final concentration) during 0–30, 0–60, 30–60, and 150–180 min of treatment. Microarray analyses were performed on three biological replicates of purified newly transcribed RNA (black bars) as well as of total RNA (empty bars) following 1 and 3 h of treatment. Bar charts depicting the number of probe sets detecting significant ($P \leq 0.05$) >4-fold up-regulation (*A*,*B*) or >2-fold down-regulation (*C*,*D*) by either IFNα or IFNγ are shown.

visualized in Fig. 4D). Interestingly, virtually all probe sets (IFNα: 86/86; IFNγ 115/119) detecting up-regulation by more than twofold in newly transcribed RNA after 30 min also revealed regulation of more than twofold at 30–60 min. Therefore, analysis of newly transcribed RNA produces highly reliable and reproducible data. Changes in transcription rates seen already during the first hour were termed "primary." This type of regulation peaked in between 30 and 60 min and mainly remained stable or started to decline thereafter. For a large part (>25%) of these transcripts changes remained undetectable in total RNA at 1 and 3 h. Additional changes seen first at 150–180 min after stimulation were termed "secondary." These also accounted for ~25% of changes. Interestingly, a large subset of genes was primary up-regulated by IFNα but secondary by IFNγ. This was remarkable as no induction of any type I IFN gene was observed during IFNγ treatment. Changes in total RNA after 1 and 3 h of IFN treatment could be quantitatively explained by corresponding changes in transcriptional activity when taking into account the half-life of the corresponding transcripts. No effect of IFN treatment on RNA stability and decay was observed.

A number of genes have been shown to be down-regulated after 6 h of IFN treatment. Little is known about the mechanisms involved (de Veer et al. 2001; Platanias 2005). Interestingly, IFNα did not lead to any substantial down-regulation of transcription during the first three hours, indicating that down-regulation observed by others following longer treatment (≥6 h; for review, see de Veer et al. 2001) is due to secondary effects. In contrast, we identified a new subset of very short-lived transcripts ($t_{1/2m}$ = 90 min) significantly down-regulated only by IFNγ following 30–60 min of treatment. These changes were almost undetectable in total RNA at 1 and 3 h when changes seen in newly transcribed RNA already waned. The half-lives of down-regulated genes were much shorter than those of up-regulated genes ($t_{1/2m}$ = 184 min; $P < 10^{-7}$). Based on direct interactions described for these genes, comprehensive interaction networks were constructed, two of them showing high connectivity (network scores of 24 and 22, respectively; see Supplemental Fig. 5A,B). It was possible to merge these two networks using direct interactions between nodes to produce a combined network comprising 21 of the 25 "focus genes" used for network analysis (Fig. 5). The majority of "focus genes" present within the networks were located within the nucleus (16 of 21). Networks showed associations with control of gene expression, cellular development, cell death, cellular growth, and proliferation.

DISCUSSION

Here, we report on a novel systemic approach to simultaneously analyze short-term changes in RNA synthesis and decay and their impact on cellular transcript levels. Labeling of newly transcribed RNA using 4sU is applicable to a large variety of cell types and organisms including humans, mice (Kenzelmann et al. 2007), and plants (Ussuf et al. 1995), as well as *Drosophila* (data not shown). It can be used for in vitro and in vivo studies since 4sU is also well tolerated by mice following i.v. injection (Kenzelmann et al. 2007). It was shown that microarray sensitivity for differential gene expression can be substantially increased by the analysis of newly transcribed RNA following two hours of labeling (Kenzelmann et al. 2007). However, in order to be able to study the temporal order of transcriptional regulation at molecular level, monitoring at much shorter time intervals is required. It was shown that incorporation of 4tU can be used to purify newly transcribed RNA from cells expressing toxoplasma gondii UPRT (Cleary et al. 2005) following as little as one hour of labeling. However, we found 4tU incorporation to be dependent on a variety of factors including cell type and UPRT expression levels (data not shown), thereby limiting short-term labeling efficiency.

In contrast, incorporation of 4sU into newly transcribed RNA seems to be predominantly concentration dependent. Therefore, labeling efficiency can be adjusted according to the desired duration of labeling and the cell type under study. We were able to achieve a density of thiolation by 4sU sufficient for in vitro biotinylation and subsequent efficient separation on magnetic beads following as little as 10 min of labeling.

We studied the response of fibroblasts to type I and II IFN to test our new approach on a well characterized template of transcriptional regulation. For the first time, we were able to determine the temporal order and kinetics of transcriptional regulation allowing differentiation of secondary signaling effects from primary ones at the time scale of minutes. In fact, >25% of IFN-induced genes differentially expressed at 3 h represented secondary signaling events. However, two major IFN-induced transcription factors (*irf1* and *socs3*) were already up-regulated by five- to eight-fold after 15 min of IFNγ treatment, emphasizing the need to study regulation of gene expression within this time scale.

Total cellular transcript levels are constantly subjected to changes in RNA synthesis and decay. Our method allows separation of total cellular RNA into newly transcribed and preexisting RNA. Thus, RNA synthesis and decay can be simultaneously analyzed in a single experimental setting. On the one hand, analysis of newly transcribed RNA allows the quantitative study of regulatory mechanisms governing transcription. This is of particular interest for subsequent promoter analyses. On the other hand, removal of newly transcribed RNA from total RNA offers a simple novel approach to determine RNA decay rates without having to block transcription. If steady-state conditions can be assumed, RNA half-life can even be determined with superior accuracy based on newly transcribed RNA/total RNA ratios alone as these offer a two order of magnitude dynamic range of measurements instead of the twofold dynamic range provided for the majority of transcripts by experiments using act-D. Thereby, precise data on RNA decay are obtained even for medium- to long-lived transcripts. As no cellular stress response is provoked, the regulatory mechanisms that govern mRNA decay, like effects exerted by miRNAs (Bhattacharyya et al. 2006), can be studied.

Calculating half-lives instead of simply attributing changes in total RNA to changes in RNA synthesis or decay as described by Kenzelmann et al. (2007) has several advantages. First, it allows quantification of the actual changes in transcript half-life. Changes in transcript half-life do not simply match changes in newly transcribed RNA/total RNA ratios. In contrast, depending on how high the actual half-life is, it may lead to substantially different

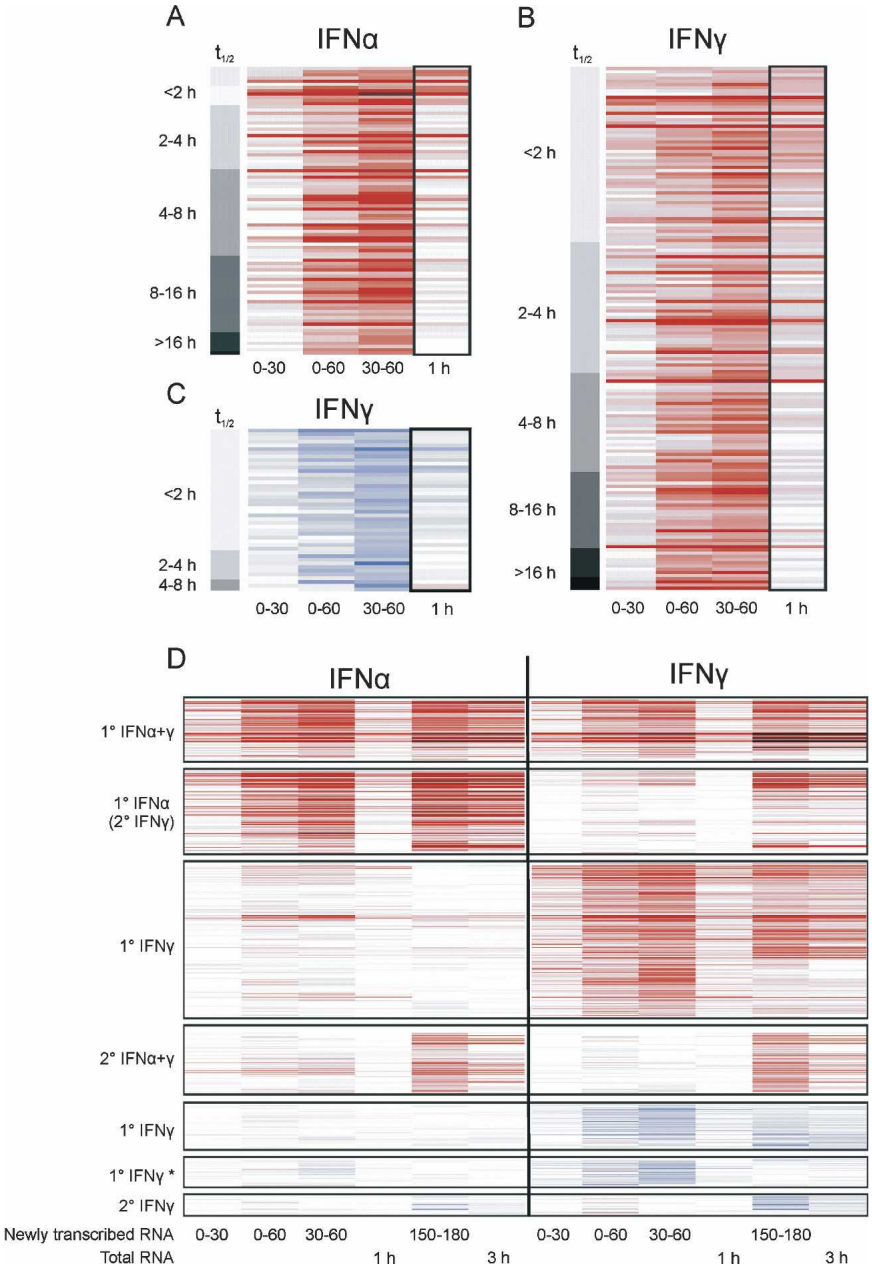

FIGURE 4. (Legend on next page)

results. Second, it allows precise analysis of both changes in RNA synthesis and decay in case both total and newly transcribed RNA levels are altered. Third, functional characteristics can be attributed to genes, e.g., genes with regulatory function are predominantly represented by short-lived transcripts. Finally, it makes data from different experiments comparable.

The most crucial step necessary to be able to compare data on RNA half-life from independent experiments is array normalization. Analysis of all three RNA subsets also provides a new solution to this problem. The standard approach is to use a housekeeping gene for which a half-life was independently determined (Frevel et al. 2003; Yang et al. 2003; Bernstein et al. 2004; Raghavan and Bohjanen 2004). Our approach is based on the concept that total RNA is quantitatively separated into newly transcribed RNA and preexisting RNA. Linear regression analysis can be applied on microarray data of thousands of transcripts. Therefore, array normalization is not dependent on the precision of the measurements of single transcripts any more but can now be based on thousands of probe sets of the actual microarray data under study.

By comparing the regulatory changes detectable for total RNA and newly transcribed RNA after 1 h of IFN treatment with transcript half-life, we show that the low temporal resolution of standard microarray analysis is due to the relatively long half-life of mammalian mRNAs. Thus, standard microarray analyses carried out on total RNA have a bias for picking up changes for short-lived transcripts. These predominantly represent regulatory genes and transcription factors creating further bias in subsequent analysis (Raghavan et al. 2002). With our approach even a transient regulation can now be revealed independent of transcript half-life. We clearly show that changes in gene expression occurring during the first hour following a stimulus are independent of transcript half-life.

Our approach is particularly well suited to detect transient down-regulation in transcription rates which is often impossible to pick up by measuring transcript abundance only. Thus, we found a new subset of short-lived genes selectively down-regulated following 30–60 min of IFNγ treatment, which was not detectable in conventional total RNA at 1 and 3 h. We show that these genes form a high connectivity functional network affecting cell cycle and apoptosis, suggesting that this response is a relevant part of IFNγ signaling. Interestingly, this response was only detectable in the second 30 min of IFN treatment. Therefore, it represents an early but potentially already secondary response specific to interferon γ.

In summary, by combining short-term analysis of RNA synthesis with simultaneous measurements of RNA decay, a comprehensive picture of the regulatory mechanism governing gene expression can be obtained.

MATERIALS AND METHODS

Cell culture and metabolic labeling of cellular RNA

Murine NIH-3T3 fibroblasts (ATCC CRL1658) were cultured in Dulbecco's modified Eagle's medium (DMEM) supplemented with 5% newborn calf serum (NCS). Human and murine cell lines including human epithelial cells (HeLa), T-cells (Jurkat), and B-cells (BL41 & DG75), as well as murine macrophages (RAW 264.7) and endothelial cells (SVEC 4-10) were cultured according to ATCC standards. For metabolic labeling of RNA in NIH-3T3 cells 4-thiouridine (Sigma) was added to 200 μM final concentration into prewarmed, CO_2-equilibrated medium in all 60-min labeling experiments (cells used only in between 5. and 15. passage after thawing; split twice weekly and 24 h before start of labeling). For short-term labeling (≤30 min), 500 μM 4sU was used. For most cell types growing in suspension (human B- and T-cells and murine macrophages) 100 μM 4sU was found to be optimal for 60-min labeling experiments (data not shown). Total cellular RNA was isolated from cells using Trizol reagent (Invitrogen) following the modified protocol described by Chomczynski and Mackey (1995).

For combined 4sU and radioactive RNA labeling 5 μM (60-min labeling with 200 μM 4sU) or 12.5 μM (15- and 30-min labeling with 500 μM 4sU) 5-^{3}H-cytidine (25 Ci/mmol, Sigma) was added to the culture media together with the 4sU. For these experiments RNA was extracted using RNeasy kit (Qiagen) to remove unincorporated 5-^{3}H-cytidine.

In order to determine mRNA decay rates by blocking transcription, act-D (Sigma) was used at a final concentration of 5 μg/mL. Both murine IFNα (IFN-αA, PBL Biomedical Laboratories) and murine IFNγ (Chemicon) were used at a final concentration of 100 U/mL in all experiments. In every experiment IFN activity was controlled using

FIGURE 4. Monitoring IFNα- and IFNγ-mediated differential gene expression. Represented are all genes which were found to be significantly regulated ($P \leq 0.01$) within any condition during the first 60 min of IFN treatment (*A–C*) or in any of the 12 statistical comparisons (*D*). Each row represents a gene, each column a biological condition. Red-to-black represents up-regulation with respect to mock-treated samples, white represents no change, and blue represents down-regulation. (*A–C*) Correlation of detectable differential gene expression with mRNA half-life. Heat-maps including genes (*A*) up-regulated by IFNα, (*B*) up-regulated by IFNγ, and (*C*) down-regulated by IFNγ by twofold for which half-life could be calculated based on newly transcribed RNA/total RNA ratios are shown. Genes were sorted according to their half-life (*top* to *bottom*). Gray scales depicted on the *left* indicate the half-life of the corresponding group of transcripts ranging from <2 to >16 h. Changes in transcript levels detectable in total RNA after 1 h of IFNα or IFNγ treatment strongly depend on the half-life of the corresponding transcript. In contrast, analysis of newly transcribed RNA revealed substantial differential expression independent of transcript half-life. (*D*) Temporal order and kinetics of IFNα- and IFNγ-mediated gene regulation. Genes were sorted by similarity (hierarchical clustering) of their regulation across four of the 12 conditions: newly transcribed RNA from 30–60 min (primary) and 150–180 min (secondary) for IFNα and IFNγ. Changes in transcription rates seen already during the first hour were termed "primary" (1°). Additional changes seen first at 150–180 min after stimulation were termed "secondary" (2°). "*" indicates transcripts down-regulated only during the first hour of IFNγ treatment with down-regulation not detectable in total RNA at 1 and 3 h at all.

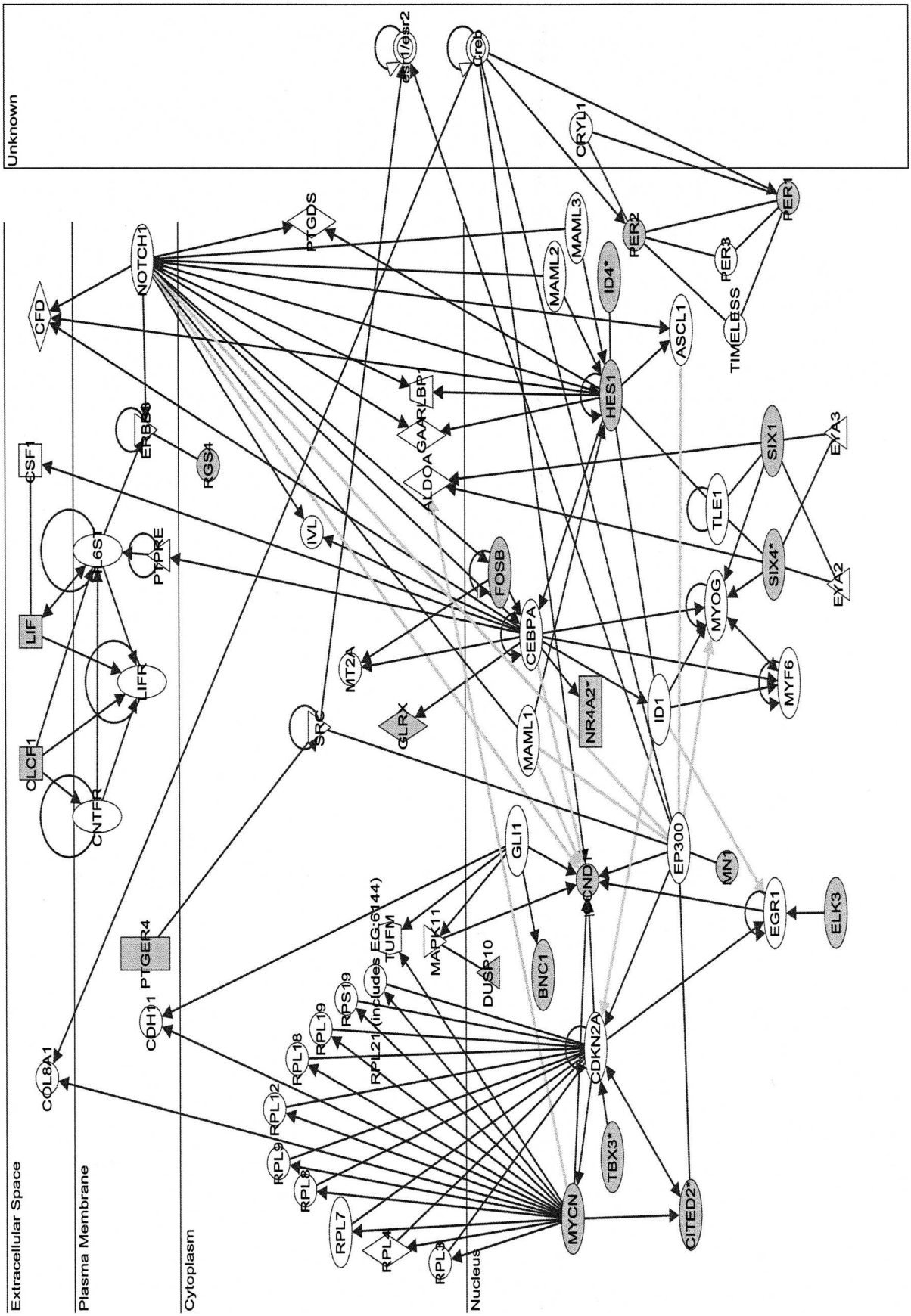

FIGURE 5. (Legend on next page)

the ISRE Luc reporter cell line, which expresses luciferase under an IFN inducible promoter (Zimmermann et al. 2005; data not shown).

Biotinylation and purification of 4sU-labeled RNA

Biotinylation of 4sU-labeled RNA was performed using EZ-Link Biotin-HPDP (Pierce) dissolved in dimethylformamide (DMF) at a concentration of 1 mg/mL and stored at 4°C. Biotinylation was carried out in 10 mM Tris (pH 7.4), 1 mM EDTA, and 0.2 mg/mL Biotin-HPDP at a final RNA concentration of 100 ng/μL for 1.5 h at room temperature. In general 50–100 μg total RNA were used for the biotinylation reaction. By dot blot assay (see below) we noted that simple precipitation of biotinylated RNA using isopropanol/ethanol as described (Cleary et al. 2005) leads to coprecipitation of large amounts of unbound biotin. As this is likely to interfere with capture of biotinylated RNA by streptavidin-coated magnetic beads we efficiently removed unbound Biotin-HPDP by chloroform/isoamylalcohol (24:1) extraction using Phase-lock-gel (Heavy) tubes (Eppendorf). Afterward, 1/10 volume of 5 M NaCl and an equal volume of isopropanol were added and RNA was precipitated at 20,000*g* for 20 min. The pellet was washed with an equal volume of 75% ethanol and precipitated again at 20,000*g* for 10 min. The pellet was resuspended in 50–100 μL RNAse-free water. After denaturation of RNA samples at 65°C for 10 min followed by rapid cooling on ice for 5 min, biotinylated RNA was captured using μMACS streptavidin beads and columns (Miltenyi). Our column-based assay eliminated the risk of carry-over of unlabeled RNA we observed when using the original protocol (Cleary et al. 2005). Up to 100 μg of biotinylated RNA were incubated with 100 μL of μMACS streptavidin beads with rotation for 15 min at room temperature. The beads were transferred and magnetically fixed to the columns. Columns were washed three times with 1 mL 65°C washing buffer (100 mM Tris-HCl, pH 7.4, 10 mM EDTA, 1 M NaCl, 0.1% Tween20) followed by three washes with room temperature washing buffer. To recover the unlabeled preexisting RNA the flow-through of the first two washes was collected and combined. Labeled RNA was eluted by the addition of 100 μL of freshly prepared 100 mM dithiothreitol (DTT) followed by a second elution round 5 min later. RNA was recovered from the washing fractions and eluates using the RNeasy MinElute Spin columns (Qiagen).

Detection of 4sU incorporation by dot blot assay

Dot blot analysis on biotinylated RNA samples was carried out to detect and quantify the amount of RNA-bound biotin residues within a given RNA sample. First, biotinylated RNA samples were denaturated for 10 min at 65°C and subsequently placed on ice for 5 min. RNA samples were diluted in ice-cold alkaline binding buffer (10 mM NaOH, 1 mM EDTA) at a concentration of 1 μg/200 μL and spotted onto a Zeta$^+$-probe blotting membrane (Bio-Rad) in 10-fold dilutions (1 μg down to 1 ng) using the Bio-Dot Apparatus (Bio-Rad). A 5′-biotinylated DNA oligo of 81 nt was used as quantitative positive control and applied to the membrane in 10-fold dilutions (100 ng down to 0.1 ng). After rinsing each well with 500 μL alkaline binding buffer, the blotting apparatus was disassembled and the membrane was incubated in blocking solution (phosphate buffered saline [PBS], pH 7.5, 10% SDS, 1 mM EDTA) for 20 min. The membrane was probed with 1:1000 dilution of 1 mg/mL streptavidin-horseradish peroxidase (Pierce) in blocking solution for 15 min. The membrane was washed six times in PBS containing decreasing concentrations of SDS (10%, 1%, and 0.1% SDS, applied twice each) for 10 min. The signal of biotin-bound horseradish peroxidase was visualized by ECL detection reagent (Amersham).

Reverse transcription and real-time PCR

Reverse transcription of 100 ng purified newly transcribed RNA was carried out in 25 μL reactions using Superscript III (Invitrogen) and oligo-dT primers (Invitrogen) following the manufacturers instructions. PCR was performed on a Light Cycler (Roche Molecular Biochemicals). Each reaction was carried out using 5 μL of cDNA (1:10 dilution) and 15 μL reaction mixtures of Light Cycler Fast Start, DNA Master^{Plus} Sybr Green I and 0.5 μM of the primers. PCRs were subjected to 10 min of 95°C hot-start, and Sybr Green incorporation was monitored for 45 cycles of 95°C denaturation for 10 sec, 58°C annealing for 3 sec, and 72°C elongation for 10 sec, followed by melting curve analysis to confirm specific amplification. The specific primer pairs for each target are listed in Supplemental Table 2. Standard curves were prepared using cDNA prepared from total RNA of NIH-3T3 cells. Relative quantification was performed based on *gapdh* normalization.

Microarray sample labeling, hybridization, and preprocessing

Total RNA (1.5 μg) and newly transcribed RNA (280 ng) were amplified and labeled using the Affymetrix One-Cycle Target Labeling Kit according to the manufacturer's recommendations. As newly transcribed RNA mainly consists of mRNA, it was amplified and labeled according to the manufacturer's protocol for mRNA. The amplified and fragmented biotinylated cRNA was hybridized to Affymetrix MG 430 2.0 arrays using standard procedures.

FIGURE 5. Combined gene network obtained based on the genes down-regulated by IFNγ treatment. Network analysis on genes selectively down-regulated at 30–60 min following IFNγ receptor activation suggested two highly connected networks when restricting to direct interactions only (see Supplemental Fig. 5A,B). Network 1 is centered on gene nodes corresponding to cyclin D1 (CDN1) and myc (MYCN) and is comprised of genes associated with protein synthesis, gene expression, and organ development. Network 2 is comprised of genes associated with cellular development, nervous system development, and gene expression functions (based on IPA Functional Analysis; see Materials and Methods for network derivation). Both networks show high connectivity (Network 1 score of 24, Network 2 score of 22) with 11 or 10 of the 35 components of each network derived from the 25 focus genes down-regulated by IFNγ (shown in gray). Interestingly, the two networks could be combined to a single network (shown) based on direct interactions of the involved genes. Direct interactions of genes within a network are shown as dark gray arrows; direct interactions of genes between networks are shown as light gray arrows. The entire list of genes contributing to both networks is provided in Supplemental Table 4.

Microarray data processing and statistical analysis for analysis of IFN-mediated gene regulation

Data were processed and analyzed with R and Bioconductor (Gentleman et al. 2004; R Development Core Team 2007). For the analysis of IFN-mediated differential gene expression processing and statistical hypothesis testing was implemented separately for total RNA and newly transcribed RNA data sets. The former contains a total of 24 arrays in seven biological conditions, the latter 36 arrays in 12 biological conditions (for details, see Supplemental Table 3).

Arrays were assessed for quality, GCRMA-normalized, filtered for low and invariant expression, and analyzed using an empirical Bayes moderated *t*-test for paired samples. Hybridization results for newly transcribed RNA and total RNA were expected and observed to show significant differences.

"Quality assessment" consisted of RNA degradation plots, Affymetrix quality control metrics, sample cross-correlation, data distributions, and probe-level visualizations.

"Normalization" incorporated (separately for each RNA type data set) background correction, normalization, and probe-level summation by GCRMA.

"Nonspecific filters" consisted of a combined intensity-based and variation-based step removing genes that can safely be considered to be biologically irrelevant or nonmeasurable by microarray technology. Filter one only retains genes which are called "present" or "marginal" in at least three out of the total number of arrays in that data set. Filter two only retains genes with a measured Inter-Quartile-Range ≥ 0.75. In the total RNA data set, $n = 4327$ genes pass this combined filter; in the newly transcribed RNA data set, this number is $n = 10{,}053$. The difference in numbers is due to the higher proportion of "present" probes in the newly transcribed RNA data set.

"Statistical testing" for differential expression was applied separately for the total RNA and newly transcribed RNA data sets. Analysis hypotheses were centered around the effect of IFNα and IFNγ at particular time points, compared to mock-treated samples. The small statistical sample size for individual biological conditions is partly offset by the paired nature of samples, in that the mock and treatment samples are the same sample with the only difference being the treatment received. This is made use of by applying a paired-test version of the empirical Bayes moderated *t*-test (Smyth 2004), which in itself is the most robust test for small sample sizes. An increased rate of false-positive results due to simultaneously testing on a large number of genes was corrected for by applying a multiple testing correction algorithm to the observed *P*-values, in this case using the Benjamini and Hochberg method (Benjamini and Hochberg 1995). Fisher's exact test was applied for comparison of the number of down-regulated genes in between IFNα and IFNγ for newly transcribed RNA.

Calculation of mRNA half-life based on newly transcribed/total RNA ratios, preexisting RNA/total RNA ratios, and actinomycin-D data

The different bioinformatical approaches used to determine RNA half-lives are described in detail in the Supplemental Methods. For all experiments three biological replicates of each RNA subset were subjected to microarray analysis.

In total this comprised 45 arrays in 11 biological conditions (for details, see Supplemental Table 3).

To calculate RNA half-lives CEL-files of all samples from all conditions (including total RNA, newly transcribed RNA, and preexisting RNA as well as the act-D RNA samples) were normalized together using the GCRMA algorithm (R Development Core Team 2007). Only probe sets called "present" in all three replicates of all three RNA subsets under study were included in the analysis of transcript half-lives. Statistical comparison of half-life values between groups was performed using the Wilcoxon rank–sum test.

Pathway analysis for genes down-regulated by IFNγ

Network analysis involved upload of gene identifier lists to the ingenuity pathway analysis (IPA) software application. The IPA Knowledge Base, a comprehensive knowledge base of biological findings for genes of human, mouse, and rat, was used to construct pathways and functional modules. The IPA application maps each gene identifier to its corresponding gene object in the IPA Knowledge Base. These focus genes are then overlaid onto a global molecular network developed from information contained in the Knowledge Base. Networks of focus genes are then algorithmically generated based on their connectivity and assigned a significance score (based on *P*-values) representing the likelihood that the focus genes within the network are found there by chance. A high number of focus genes within a data set leads to a higher network score (equal to the negative exponent of the respective *P*-value). To identify focus genes down-regulated after IFNγ treatment, the database was queried using the 44 probe IDs present in this list and 25 focus genes were identified as eligible for network analysis. Comprehensive interaction networks were constructed showing high connectivity (Network 1 score of 24 and Network 2 score of 22; for details, see Supplemental Fig. 5A,B).

SUPPLEMENTAL DATA

Supplemental material can be found at http://www.rnajournal.org.

ACKNOWLEDGMENTS

We thank Angela Servatius for her excellent technical assistance, Klaus Conzelmann for his help and advice with setting up the IFN experiments, and Steven Watterson for proofreading the mathematic sections. This work was funded by NGFN grants 01GS0405 (to U.H.K.) and FKZ 01G0113 TP 37 (to R.H.) as well as grants for a Centre for Integrative Systems Biology supported by BBSRC and EPSRC, FP6 InfoBioMed programme and Wellcome Trust (to P.G.). L.D., Z.R., and U.H.K. designed the study and wrote the paper. L.D. and B.R. performed the experiments. L.D., C.C.F., and R.Z. developed and C.C.F. implemented the new bioinformatics approach used to calculate mRNA half-lives from the experimental results. R.H. and J.M. provided the microarray data at the TUM microarray facility with the help of Angela Servatius and contributed to data analysis. P.D., T.F. and P.G. helped with array study design, analyzed the microarray data, and performed pathway analysis for IFN regulation.

Received April 14, 2008; accepted May 27, 2008.

REFERENCES

Benjamini, Y. and Hochberg, Y. 1995. Controlling the false discovery rate: A practical and powerful approach to multiple testing. *J. R. Stat. Soc. Ser. B Methodol.* **57:** 289–300.

Bernstein, J.A., Khodursky, A.B., Lin, P.H., Lin-Chao, S., and Cohen, S.N. 2002. Global analysis of mRNA decay and abundance in *Escherichia coli* at single-gene resolution using two-color fluorescent DNA microarrays. *Proc. Natl. Acad. Sci.* **99:** 9697–9702.

Bernstein, J.A., Lin, P.H., Cohen, S.N., and Lin-Chao, S. 2004. Global analysis of *Escherichia coli* RNA degradosome function using DNA microarrays. *Proc. Natl. Acad. Sci.* **101:** 2758–2763.

Bhattacharyya, S.N., Habermacher, R., Martine, U., Closs, E.I., and Filipowicz, W. 2006. Relief of microRNA-mediated translational repression in human cells subjected to stress. *Cell* **125:** 1111–1124.

Boxel-Dezaire, A.H., Rani, M.R., and Stark, G.R. 2006. Complex modulation of cell type-specific signaling in response to type I interferons. *Immunity* **25:** 361–372.

Chomczynski, P. and Mackey, K. 1995. Short technical reports. Modification of the TRI reagent procedure for isolation of RNA from polysaccharide- and proteoglycan-rich sources. *Biotechniques* **19:** 942–945.

Cleary, M.D., Meiering, C.D., Jan, E., Guymon, R., and Boothroyd, J.C. 2005. Biosynthetic labeling of RNA with uracil phosphoribosyltransferase allows cell-specific microarray analysis of mRNA synthesis and decay. *Nat. Biotechnol.* **23:** 232–237.

de Veer, M.J., Holko, M., Frevel, M., Walker, E., Der, S., Paranjape, J.M., Silverman, R.H., and Williams, B.R. 2001. Functional classification of interferon-stimulated genes identified using microarrays. *J. Leukoc. Biol.* **69:** 912–920.

Fan, J., Yang, X., Wang, W., Wood III., W.H., Becker, K.G., and Gorospe, M. 2002. Global analysis of stress-regulated mRNA turnover by using cDNA arrays. *Proc. Natl. Acad. Sci.* **99:** 10611–10616.

Frevel, M.A., Bakheet, T., Silva, A.M., Hissong, J.G., Khabar, K.S., and Williams, B.R. 2003. p38 Mitogen-activated protein kinase-dependent and -independent signaling of mRNA stability of AU-rich element-containing transcripts. *Mol. Cell. Biol.* **23:** 425–436.

Garcia-Martinez, J., Aranda, A., and Perez-Ortin, J.E. 2004. Genomic run-on evaluates transcription rates for all yeast genes and identifies gene regulatory mechanisms. *Mol. Cell* **15:** 303–313.

Gentleman, R.C., Carey, V.J., Bates, D.M., Bolstad, B., Dettling, M., Dudoit, S., Ellis, B., Gautier, L., Ge, Y., Gentry, J., et al. 2004. Bioconductor: Open software development for computational biology and bioinformatics. *Genome Biol.* **5:** R80. doi: 10.1186/gb-2004-5-10-r80.

Guhaniyogi, J. and Brewer, G. 2001. Regulation of mRNA stability in mammalian cells. *Gene* **265:** 11–23.

Hirayoshi, K. and Lis, J.T. 1999. Nuclear run-on assays: Assessing transcription by measuring density of engaged RNA polymerases. *Methods Enzymol.* **304:** 351–362.

Jing, Q., Huang, S., Guth, S., Zarubin, T., Motoyama, A., Chen, J., Di Padova, F., Lin, S.C., Gram, H., and Han, J. 2005. Involvement of microRNA in AU-rich element-mediated mRNA instability. *Cell* **120:** 623–634.

Kenzelmann, M., Maertens, S., Hergenhahn, M., Kueffer, S., Hotz-Wagenblatt, A., Li, L., Wang, S., Ittrich, C., Lemberger, T., Arribas, R., et al. 2007. Microarray analysis of newly synthesized RNA in cells and animals. *Proc. Natl. Acad. Sci.* **104:** 6164–6169.

Liu, B., Yang, Y., Chernishof, V., Loo, R.R., Jang, H., Tahk, S., Yang, R., Mink, S., Shultz, D., Bellone, C.J., et al. 2007. Proinflammatory stimuli induce IKKalpha-mediated phosphorylation of PIAS1 to restrict inflammation and immunity. *Cell* **129:** 903–914.

Melvin, W.T., Milne, H.B., Slater, A.A., Allen, H.J., and Keir, H.M. 1978. Incorporation of 6-thioguanosine and 4-thiouridine into RNA. Application to isolation of newly synthesised RNA by affinity chromatography. *Eur. J. Biochem.* **92:** 373–379.

Platanias, L.C. 2005. Mechanisms of type-I- and type-II-interferon-mediated signalling. *Nat. Rev. Immunol.* **5:** 375–386.

R Development Core Team 2007. A language and environment for statistical computing. ISBN 3-900051-07-0. http://www.R-project.org. 2007.

Raghavan, A. and Bohjanen, P.R. 2004. Microarray-based analyses of mRNA decay in the regulation of mammalian gene expression. *Brief. Funct. Genomic. Proteomic.* **3:** 112–124.

Raghavan, A., Ogilvie, R.L., Reilly, C., Abelson, M.L., Raghavan, S., Vasdewani, J., Krathwohl, M., and Bohjanen, P.R. 2002. Genome-wide analysis of mRNA decay in resting and activated primary human T lymphocytes. *Nucleic Acids Res.* **30:** 5529–5538.

Shyu, A.B., Greenberg, M.E., and Belasco, J.G. 1989. The c-fos transcript is targeted for rapid decay by two distinct mRNA degradation pathways. *Genes & Dev.* **3:** 60–72.

Smyth, G.K. 2004. Linear models and empirical bayes methods for assessing differential expression in microarray experiments. *Stat. Appl. Genet. Mol. Biol.* **3:** Article3.

Stetson, D.B. and Medzhitov, R. 2006. Type I interferons in host defense. *Immunity* **25:** 373–381.

Ussuf, K.K., Anikumar, G., and Nair, P.M. 1995. Newly synthesised mRNA as a probe for identification of wound responsive genes from potatoes. *Indian J. Biochem. Biophys.* **32:** 78–83.

Woodford, T.A., Schlegel, R., and Pardee, A.B. 1988. Selective isolation of newly synthesized mammalian mRNA after in vivo labeling with 4-thiouridine or 6-thioguanosine. *Anal. Biochem.* **171:** 166–172.

Yang, E., van Nimwegen, E., Zavolan, M., Rajewsky, N., Schroeder, M., Magnasco, M., and Darnell Jr., J.E. 2003. Decay rates of human mRNAs: Correlation with functional characteristics and sequence attributes. *Genome Res.* **13:** 1863–1872.

Zimmermann, A., Trilling, M., Wagner, M., Wilborn, M., Bubic, I., Jonjic, S., Koszinowski, U., and Hengel, H. 2005. A cytomegaloviral protein reveals a dual role for STAT2 in IFN-γ signaling and antiviral responses. *J. Exp. Med.* **201:** 1543–1553.

Metabolic tagging and purification of nascent RNA: implications for transcriptomics

Caroline C. Friedel*[a] and Lars Dölken[b]

Received 10th June 2009, Accepted 27th July 2009
First published as an Advance Article on the web 26th August 2009
DOI: 10.1039/b911233b

Gene expression profiling to analyze cellular responses against different stimuli or conditions is generally performed at the total cellular RNA level. This results in poor resolution of the temporal kinetics of the cellular response and a bias towards detecting up-regulation of short-lived transcripts. Furthermore, changes in transcription rate and RNA stability cannot be distinguished. These problems can be addressed by analyzing nascent RNA instead of total cellular RNA. Throughout the last few years methods have been developed for metabolic tagging and purification of nascent RNA. In this article, we review these experimental procedures and discuss their implications for large-scale gene expression profiling.

Introduction

During the cell cycle and in response to different stimuli cells continuously alter their gene expression program. This requires the coordinated and cooperative interplay of a large variety of biological processes. At the RNA level it includes recruitment of RNA polymerases, initiation, elongation and termination of transcription, RNA processing, transport and translation as well as RNA decay. Thus, for every transcript, total RNA levels are the result of a fine-tuned balance between RNA synthesis and RNA decay. In the last couple of years high-throughput technologies have been successfully applied to study these processes. Whole-genome microarrays and high-throughput sequencing (ChIP-seq, RNA-Seq) allow the study of chromatin structure, recruitment of transcription factors and polymerase activity as well as the measurement of total RNA levels and RNA decay on whole transcriptome level.[1–5] As all of these processes affect the total cellular RNA, it is most commonly used to study the effect of a given condition or stimuli. While studies on total cellular RNA usually result in the identification of hundreds of differentially expressed genes, the underlying mechanisms often remain concealed. This is mainly due to the following three reasons. First, by analyzing total cellular RNA the detected changes cannot be easily attributed to alterations in RNA synthesis or decay. Therefore, the fundamental character of the alteration often remains elusive unless studied by additional means. Second, fold changes detectable in total RNA do not simply reflect changes in RNA synthesis but are substantially dependent on differences in transcript turnover between genes. For instance, a 20-fold induction of a long-lived transcript (*e.g.* $t_{1/2}$ = 24 h) only results in a ~1.5-fold increase in total RNA levels after 1 h but in a >15-fold induction for a

[a] *Institute for Informatics, Ludwig-Maximilians-University Munich, Amalienstr. 17, 80333 München, Germany. E-mail: caroline.friedel@bio.ifi.lmu.de; Fax: +49-89-2180-99-4056; Tel: +49-89-2180-4056*
[b] *Max von Pettenkofer-Institute, Ludwig-Maximilians-University Munich, Pettenkoferstraße. 9a, 80336 München, Germany. E-mail: doelken@mvp.uni-muenchen.de; Fax: +49-89-5160-5292; Tel: +49-89-5160-5290*

Caroline C. Friedel

Caroline C. Friedel obtained her PhD in computational biology in 2009 from the Ludwig-Maximilians-University of Munich, Germany. She performed her thesis work in the Bioinformatics group of Ralf Zimmer at the Institute for Informatics and is currently a postdoctoral fellow in the same group. Her research interests include interactomics, protein complex structure and regulation and the development of new computational approaches to gene expression profiling based on nascent RNA.

Lars Dölken

Lars Dölken studied human medicine at the Ernst-Moritz-Arndt-University of Greifswald and the University of Otago, Dunedin, New Zealand. After completing his MD PhD in haematology/oncology at the University of Greifswald he is currently a postdoctoral fellow in the laboratory of Professor Ulrich H. Koszinowski at the Max von Pettenkofer-Institute in Munich, Germany. Here, he is studying the role of herpes virus miRNAs and developing new methods for high resolution gene expression profiling.

short-lived transcript (*e.g.* $t_{1/2}$ = 30 min). Similarly, the complete shut-down in RNA synthesis of an average-lived transcript ($t_{1/2}$ = 5 h) takes 5 h to result in a two-fold reduction in the total RNA level. Therefore, the true changes in transcriptional activity are obscured by differences in transcript half-life. This is a major problem in any subsequent analysis (*e.g.* promoter analyses) as the extent of transcriptional regulation cannot be properly quantified.

Third, due to the low sensitivity of gene expression analysis on total RNA, the temporal resolution for detecting changes in gene expression by analyzing total cellular RNA is rather poor. In order to increase the detection level for differentially expressed genes the total cellular RNA level is usually analyzed many hours after the stimulus was applied. At this time multiple molecular mechanisms including a broad spectrum of secondary signaling events contribute to the observed changes, particularly for short-lived genes. In consequence, the underlying mechanisms cannot easily be dissected.

Recent improvements in metabolic tagging of newly transcribed (nascent) RNA and downstream purification techniques provide new solutions to these problems. Here, we review the experimental techniques currently available to tag and isolate nascent RNA. In addition, their advantages and the new opportunities they offer for analyzing the kinetics and regulation of differential RNA synthesis and decay are discussed.

Analysis of transcriptional activity by nuclear run-on assays (NRO)

The basic limitations of analyzing only total RNA have long been recognized. Nevertheless, total cellular RNA is still most commonly used to study differential gene expression. When only studying the expression of a small number of genes nuclear run-on assays (NRO) have long been the method of choice to evaluate transcriptional activity and the relative contributions of RNA synthesis and turnover.[6–8] Briefly, nuclei are isolated after rapid cooling. By restoring physiological temperature conditions and adding radio-labeled as well as endogenous nucleotides, transcriptionally engaged polymerases resume elongation. Depending on the time of nuclear run-on the incorporated radio-label is restricted to sequences of defined length immediately downstream of the engaged polymerases. Total RNA is then isolated and hybridized to probes on macroarrays to detect transcript sequences of interest based on the incorporated radio-labeled nucleotides.[8,9] Therefore, NROs measure the density of transcribing RNA polymerases over specific target regions of the genome and are able to map the position of these polymerases with high precision. Thus, they can provide reasonable approximations for transcription rates and kinetics for some genes. Unfortunately, these methods are cell-invasive and, until recently, were not compatible with current microarray formats.

Compatibility was achieved by the recent work of Core *et al.*[10] They combined NRO with a ribonucleotide analogue [5-bromouridine 5′-triphosphate (BrUTP)] to BrU-tag nascent RNA during the run-on step (Fig. 1A). NRO-RNA was immunoprecipitated and then sequenced using Illumina high-throughput sequencing technology. Thus, they were able to map transcriptional activity of RNA polymerases with high resolution. Interestingly, they found that >13 000 genes (55% of all genes, 77% of active genes) displayed significant transcription within 1 kb upstream of sense-oriented promoter-proximal peaks. It remains unclear whether this widespread transcriptional activity that lies upstream but opposite to the direction of coding genes positively or negatively regulates transcription output and how productive elongation in one direction *versus* the other is distinguished.

Two aspects still limit the general applicability of this approach. First, the procedure is technically demanding. It requires isolation of nuclei which is notoriously difficult for some cell types (*e.g.* lymphocytes). Second, NRO-RNA is only transcribed *in vitro* following isolation of nuclei, a condition potentially causing experimental bias. Recently, it was shown that BrU can also be used to directly tag nascent RNA in living cells.[11] BrU is added to cell culture medium followed by the isolation of tagged RNA by immunoprecipitation using a mouse anti-bromodeoxyuridine antibody coupled to goat anti-mouse IgG Dynabeads (Fig. 1B). While this approach seems to be generally applicable and yields nascent RNA of high purity, BrU toxicity, BrU incorporation rates and the efficiency of capturing BrU-tagged RNAs in particular for transcripts with low uridine content remain to be addressed.

Metabolic tagging of nascent RNA using thiol-modified nucleosides

Background

It has been known for more than 30 years that thiol-containing nucleosides like 4-thiouridine are readily incorporated into nascent RNA with minimal toxic effects.[12] Two studies published in 1977 and 1978 showed that 2-thiouridine, 4-thiouridine and 6-thioguanine are incorporated into nascent RNA by mammalian cells.[12,13] Following short-term exposure of 30–60 min none of the three nucleoside analogues significantly affect RNA and protein synthesis. After longer periods of exposure, the cytotoxic effect of 6-thioguanosine results in impaired synthesis of both RNA and protein.[12,14] Proteins synthesized after treatment of cells with 6-thioguanosine are less stable due to misincorporated amino acids resulting in disruption of protein folding. In contrast, even after long exposure (>24 h) to high concentrations of 4-thiouridine, synthesis and decay of both nascent RNA and proteins are not significantly affected. Although the advantage of being able to isolate and analyze nascent RNA lies at hand, the value of this technique was not broadly recognized during the next 25 years. Only three studies on transcriptional regulation in human T-cells, hamster cells and potato plants confirmed the data of the initial studies.[14–16]

RNA tagging using 4-thiouracil (4tU)

Cleary *et al.* were the first to combine a thiol-mediated RNA tagging approach with current high-throughput technologies.[17,18] Instead of 4-thiouridine (4sU) they used 4-thiouracil (4tU) which, in addition to cellular pyrimidine kinases, requires the enzyme activity of a uracil phosphoribosyltransferase (UPRT). In many

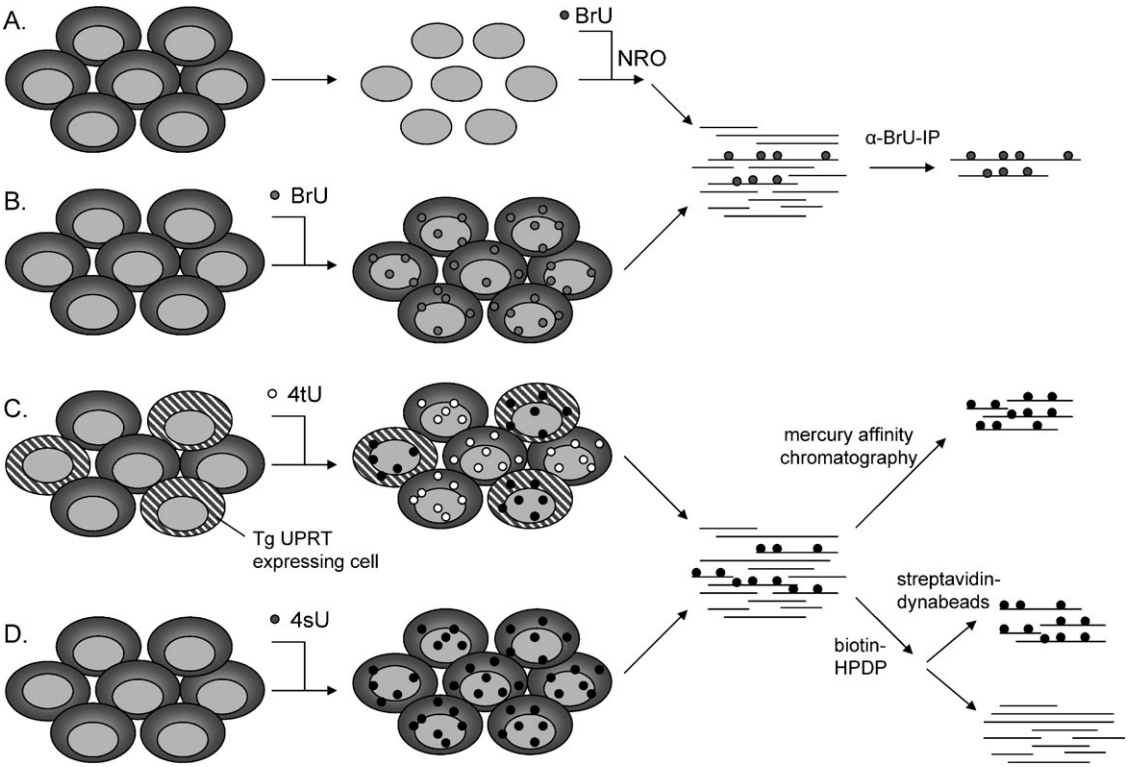

Fig. 1 Methods for metabolic tagging and purification of nascent RNAs. (A and B) Anti-BrU immunoprecipitation of nascent RNA following (A) nuclear run-on assay (NRO) using BrU (symbols: cells (dark grey) and nuclei (light grey)) or (B) metabolic tagging of living cells using BrU. (C) Thiol-mediated purification of nascent RNA following 4tU-tagging of nascent RNA selectively in cell expressing *T. gondii* UPRT (Tg UPRT). (D) 4sU-tagging of nascent RNA in all cells. 4tU (empty circle) is only activated to 4t-uridinetriphosphate (4t-UTP = black circle) in cells expressing Tg UPRT whereas 4sU (dark grey circle) is activated to 4t-UTP in all cells. Thiol-labeled RNA can then either be purified using mercury affinity chromatography or thiol-specifically biotinylated (biotin-HPDP) and separated from untagged pre-existing RNA using streptavidin coated magnetic beads.

organisms UPRT is the key enzyme for a pyrimidine salvage pathway recycling uracil to uridine monophosphate using phosphoribosyl pyrophosphate (PRPP). However, this salvage pathway is not present in mammalian or insect cells.[17,19] UPRT enzymes of different organisms vary in their substrate specificity. So far, only UPRT of the protozoa *Toxoplasma gondii* (Tg UPRT) and of yeast have been found to be able to utilize 4tU as an additional substrate (Fig. 1C). However, by introducing Tg UPRT into mammalian cells this pathway can be successfully established.[17] Cleary *et al.* also replaced the mercury affinity chromatography based purification assay by a simple protocol based on thiol-specific biotinylation (using Biotin HPDP) of thiol-labeled RNA followed by isolation of nascent RNA using streptavidin coated magnetic beads. Following 1 h of 4tU treatment high quality nascent RNA was recovered in sufficient amounts from *T. gondii* cultures and Tg UPRT transduced HELA cells to perform microarray analysis. By injecting mice infected with *T. gondii* i.v. with 4tU they were even able to selectively tag and purify nascent RNA from the parasite *in vivo* thereby demonstrating that 4tU-tagging and purification of nascent RNA is also applicable for *in vivo* studies.

A major problem for gene expression profiling from complex tissues *in vivo* is the presence of a large number of different cell types. However, the changes of interest may occur only in a single cell type. Thus, this response is masked by the presence of other cell types. In addition, alterations of tissue composition, *e.g.* immigration of inflammatory cells, may substantially alter RNA profiles leading to a significant experimental bias which is nearly impossible to dissect. Numerous attempts have been undertaken to solve this problem, *e.g.* using laser dissection of complex tissue, cell sorting or single cell microarray analysis,[20–23] all of which are notoriously laborious, difficult to establish and not generally applicable. As 4tU-tagging is dependent on the presence of adequate levels of Tg UPRT in the cells of interest, cell type specific tagging of nascent RNA can be achieved by expressing Tg UPRT under the control of a cell type specific promoter or by using conditional systems. By spatially restricting UPRT expression in *Drosophila*, Miller *et al.* recently demonstrated that 4tU is modified and subsequently incorporated into newly synthesized RNA only in cells expressing UPRT.[19] Thus, after isolating total cellular RNA from an organ or even the whole organism, 4tU-tagged RNA from Tg UPRT expressing cells can be specifically purified. As this method appears to be generally applicable to a large number of model organisms, it is likely to prove valuable *e.g.* for studies on embryonic development.

Viruses can also be engineered to express Tg UPRT in order to selectively tag and purify RNA from virus infected cells. While we found this approach to work nicely in fibroblasts infected with a murine cytomegalovirus mutant expressing Tg UPRT *in vitro*, the efficiency of RNA tagging varied between

different cell types despite similar levels of Tg UPRT expression (unpublished data). This may reflect differences in PRPP levels in between cell types but still requires further studies. Further problems which need to be solved to apply 4tU/Tg UPRT based RNA tagging as a standard method to tag nascent RNA in specific cells *in vivo* are the impurity of RNA samples from solid organs, such as the liver, and the toxicity of solvents required to solubilize 4tU (*e.g.* DMSO).

RNA tagging using 4-thiouridine (4sU)

In contrast to 4-thiouracil (4tU), incorporation of 4-thiouridine (4sU) into nascent RNA only requires the activity of ubiquitous nucleoside kinases. Therefore, this approach is more readily applicable for *in vitro* studies. In contrast to 4tU, 4sU is easily dissolved in water or phosphate buffered saline (PBS). Furthermore, intravenous injection of mice with 4sU is tolerated without any detectable toxic effects (unpublished data). Studying a mouse ischaemia model, Kenzelmann *et al.* successfully applied this approach to mice by injecting 4sU intraperitoneally (i.p.) into mice and isolating nascent RNA using the organo-mercury affinity chromatography based approach (Fig. 1D).[24] Applying both purified nascent and total RNA to Affymetrix microarrays they showed that analysis of nascent RNA following two hourly i.p. injections with 1 ml 200 μM 4sU resulted in a ~10-fold increase in microarray sensitivity and allowed differentiation of changes in RNA synthesis from alterations in RNA decay. We recently developed an improved integrated approach which combines the advantages of direct incorporation of 4sU with thiol-specific biotinylation and magnetic separation of total RNA into nascent and pre-existing untagged RNA with high purity (Fig. 1D).[25] This allows the parallel quantification of all three RNA subsets by microarrays or RNA sequencing. The untagged pre-existing RNA is very similar to RNA obtained following transcriptional arrest following actinomycin-D treatment. Thus, RNA turnover rates and changes in both RNA decay and synthesis as well as their impact on total RNA levels can be analyzed in a single experimental setting.

Comparison of 4sU- with 4tU-based tagging

RNA tagging can be started at any time point during an experiment by adding 4sU or 4tU to cell culture medium. Therefore, temporal kinetics of transcriptional changes can be analyzed by addition of 4sU or 4tU to cell culture medium at different time points following the stimulus. In contrast to 4tU tagging, which we found to be predominantly dependent on Tg UPRT activity (and potentially PRPP levels), incorporation of 4sU into nascent RNA is highly correlated with the applied 4sU concentration.[25] We found this to be comparable for a broad range of human and murine cell lines including fibroblasts, endothelial cells, B- and T-cells, macrophages and dendritic cells. In general, it appeared that cells growing in suspension required about 2-fold lower 4sU concentrations to achieve a similar tagging density than adherent cells. This may be due to a larger surface/volume ratio of cells growing in suspension thereby promoting 4sU uptake from the medium. In addition, we found 4sU tagging to also work well in *Drosophila* and *Xenopus* cells.

In mammalian cells 4sU is rapidly taken up by cells just like other nucleosides, with intra- and extracellular levels probably equalizing within less than a minute. After entering a cell 4sU is rapidly phosphorylated by cellular uridine kinases thereby preventing 4sU exit by adding a negative charge. In consequence, phosphorylated 4sU is continuously accumulating in cells over time, thereby increasing tagging efficiency. Therefore, the 4sU concentration needs to be adjusted depending on the duration of tagging. In general, a higher concentration of 4sU (500 μM to 5 mM 4sU) will improve tagging and capture efficacy for short (≤30 min) and ultra-short (≤5 min) tagging. For longer tagging periods (>1 h) lower concentrations (50 to 200 μM 4sU) should be preferred to prevent metabolic stress due to excessive 4sU incorporation. Following purification of 4sU/4tU-tagged nascent RNA the thiol-content can be directly quantified by spectrophotometric measurements by specific absorption of light at 330 nm.

Poor incorporation of 4sU/4tU into nascent RNA may affect the efficiency of capturing short transcripts with few uracil residues thereby creating an experimental bias. This is particularly important when comparing nascent RNA levels with total RNA levels to determine RNA half-lives (see below) or compare nascent RNA levels from different organs *in vivo*. Miller *et al.*[19] recently reported such a bias when analyzing nascent RNA isolated from glia cells in *Drosophila*. Here, transcripts with less than ~500 uracil residues were captured with significantly lower efficiency (up to >4× lower). This bias was then corrected for by computational means. In contrast, we observed no significant transcript size bias when analyzing nascent RNA following 1 h 4sU tagging in human B-cells (100 μM 4sU) and murine fibroblasts (200 μM 4sU).[26] Thus, also short transcripts (200–500 nt) can be captured with high efficiency. For very short transcripts (<200 nt) capture efficiency needs to be corrected for by computation means. This will be particularly important if RNA tagging is applied to detect small non-coding RNAs such as, *e.g.* snoRNAs.

While 4sU/4tU tagged RNA is compatible with microarray analysis, its compatibility with high-throughput sequencing technologies may be a point of concern. We found 4sU-containing nascent RNA prepared from human B-cells following as little as 5 min of 4sU tagging to provide reliable and reproducible results in RNA-Seq (SOLiD; in corporation with Applied Biosystems; unpublished observations). One of the first steps during sample preparation for both microarray analysis and high-throughput sequencing is cDNA synthesis. Here, 4sU incorporation does not result in altered base pairing and subsequent sequence errors. As cDNA prepared from nascent RNA is then free of 4sU, nascent RNA appears to be fully compatible with next generation sequencing technologies.

Cells can be cultured in the presence of 100 μM 4sU for >24 h without gross toxic effects. No effect of 4sU treatment was detectable in total RNA in murine fibroblasts by microarray analysis following up to 2 h of 200 μM 4sU treatment.[24,25] The lack of effects even on short-lived transcripts strongly argues against any significant, general and direct short-term effect of 4sU incorporation on RNA decay in fibroblasts. As tagging can be restricted to as little as 5–15 min we believe that any experimental bias on RNA synthesis and decay caused by 4sU treatment is minimal.

Comparison of gene expressing profiling on total and nascent RNA

Increasing sensitivity and resolving temporal kinetics

Due to the relatively long half-life of the majority of transcripts (5–10 h for mammalian cells[5,25]), basal transcription rates are low. For a transcript with a half-life of 10 h the fraction of transcripts that are newly synthesized within one hour is only ~7%. Therefore, even a 10-fold induction only leads to a ~1.6- and ~2.2-fold increase in total RNA levels after 1 and 2 h, respectively (Fig. 2A).

Accordingly, even a complete shut-down of transcription only leads to a 2-fold reduction after 10 h (Fig. 2B). In contrast, for a short-lived transcript with a half-life of *e.g.* 1 h, the same changes in transcription lead to rapid and strong up- or down-regulation detectable in total RNA. Transcript half-lives and corresponding synthesis rates are usually not considered when interpreting changes detected in total RNA. However, a 1.5-fold increase of a long-lived transcript may be highly significant because it reflects a large induction of synthesis rate, while the same fold-change for a short-lived transcript does not. Unfortunately, changes in transcription rates cannot be simply calculated from changes in total RNA abundance using transcript half-life. As even large changes in transcription only lead to small changes in total RNA for medium- to long-lived transcripts, small measurement errors are misinterpreted as large changes in RNA transcription for these transcripts (Fig. 3A).

Even strong changes in transcription rates of medium- to long-lived transcripts hardly affect total RNA levels within the first hour (Fig. 2). Therefore, looking for short-term changes in total RNA levels has a strong bias for detecting up-regulation of short-lived RNAs.[25] As many transcription factors and genes involved in regulation of biological processes have a short transcription half-life[5,26,27] this also creates additional bias in downstream analysis. In fact, a number of studies have reported that various stimuli, *e.g.* cytokine treatment, result in a selective induction of regulatory genes and transcription factors during the first hour. Contrary to that, differentially expressed genes detected in nascent RNA show no such bias towards short transcript half-life.[25] As alterations in transcription rate immediately affect nascent RNA levels, differentially expressed genes can be detected within minutes following a stimulus.[25] For instance, following treatment of murine

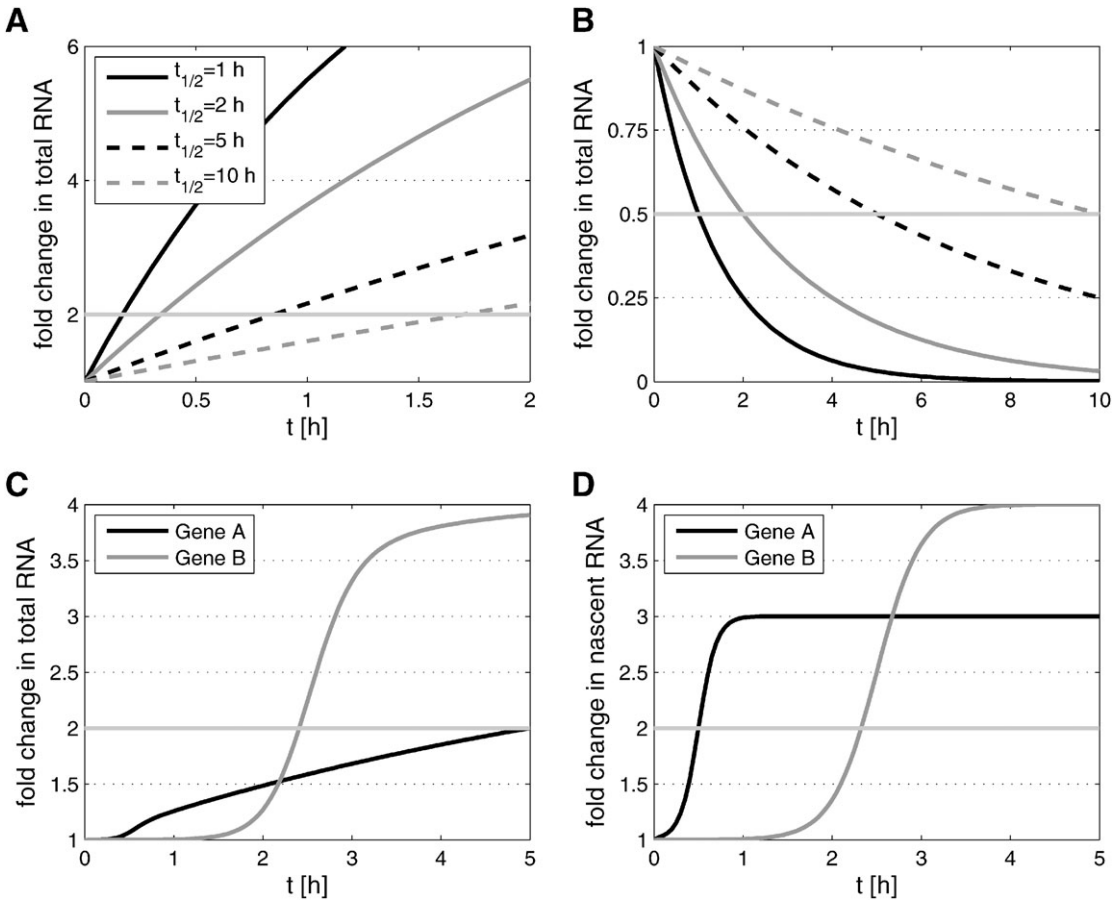

Fig. 2 Temporal delay between changes in transcription rate and changes in total RNA. (A) Changes in total RNA levels in the first 2 h following a 10-fold induction in gene expression are shown for genes with a transcript half-life of 1, 2, 5 and 10 h. The light grey horizontal line indicates a 2-fold change in total RNA levels. (B) Changes in total RNA after complete transcriptional arrest are shown for genes with a half-life of 1, 2, 5 and 10 h. (C and D) Resolution of temporal kinetics in total and nascent RNA. While the primary response for a long-lived transcript (gene A, $t_{1/2}$ = 10 h) and the secondary response for a short-lived transcript (gene B, $t_{1/2}$ = 2 h) cannot be accurately distinguished in total RNA (C), the temporal development of the cell response can be identified in nascent RNA (D).

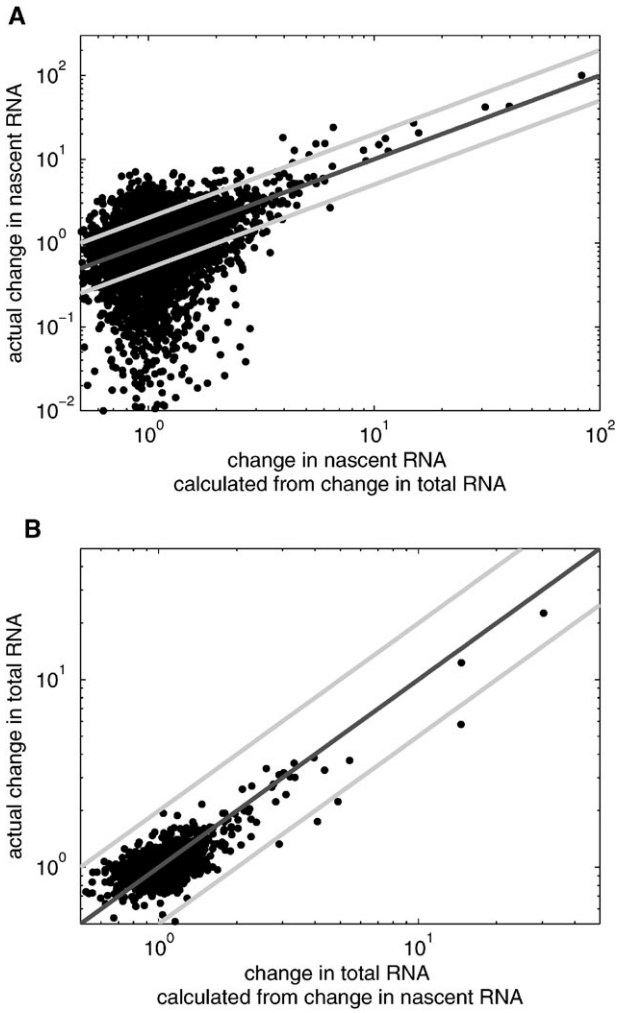

Fig. 3 Correlating observed and expected changes in transcription and total RNA abundance using transcript half-life. (A) Observed changes in nascent RNA after 1 h of IFNγ treatment[25] were compared to changes expected from changes in total RNA abundance based on transcript half-life. As small measurement errors may be misinterpreted as large transcription changes in particular for long-lived transcripts, transcription changes cannot be determined confidently from changes in total RNA. In contrast, changes in total RNA can be determined with high precision from nascent RNA (B).

fibroblasts with IFNγ a ~8- and ~5-fold induction of interferon regulatory factor 1 (irf1) and suppressor of cytokine signaling 3 (socs3) could already be detected after 15 min, respectively. The rapid induction of these two major regulators emphasizes the need to study regulatory changes in the time scale of minutes instead of hours. In this study on interferon-induced genes, sensitivity for detection of up- and down-regulation could be increased by 5- to 7-fold and 10-fold, respectively, by analyzing nascent RNA instead of total RNA.[25] Similarly, when studying serum-starvation of primary mouse embryonal fibroblast cells, Kenzelmann *et al.* identified only 50 differentially expressed genes in total RNA but 247 in nascent RNA.[24]

Due to the long delay between changes in transcription rates and noticeable changes in total RNA abundance, in particular for stable transcripts, the temporal resolution of gene expression studies on total cellular RNA is necessarily low and primary effects cannot be distinguished from secondary downstream effects of the first primary response. In consequence, secondary changes in short-lived transcripts may be observed even earlier in total RNA than the primary changes of long-lived transcripts (Fig. 2C). Thus, even serial measurements of total RNA over time cannot elucidate the true kinetics of the cell response. Contrary to that, the true kinetics of the reaction of the cell can be easily monitored in nascent RNA (Fig. 2D). Furthermore, as 4sU treatment can be started at any point independent of the stimulus under study, potential toxic effects of 4sU can be easily avoided by short-term tagging at selected time points.[25] These data clearly demonstrate that the analysis of nascent RNA allows both a more sensitive and unbiased detection of differentially expressed genes. Thus, the temporal kinetics of the cell response to stimuli and to changes in conditions can be studied, and primary and secondary responses can be distinguished.

Differentiation of changes in RNA synthesis and decay

Although analysis of total RNA can identify differentially expressed genes, it cannot distinguish whether these are due to changes in transcription rate, RNA decay or a combination of both. This can be achieved when analyzing both total and nascent RNA. Differences in nascent RNA levels which may not always be confirmed in total RNA indicate changes in transcription rate while changes in total RNA levels without a corresponding change in nascent RNA indicate altered RNA stability. In the study by Kenzelmann *et al.* which compared serum-starved and serum-induced mouse embryonic fibroblasts, 30 of 50 genes with altered expression levels in total RNA following 2 h of serum and 4sU treatment showed no significant changes in nascent RNA.[24] qRT-PCR analysis of these genes confirmed that the changes in total RNA most likely resulted from altered RNA stability. However, this approach is not easily applicable when both total and nascent RNA levels are altered. In addition, a lack of RNA stability may already affect nascent RNA levels following 2 h of tagging. A possible solution to this problem is to compare observed changes of nascent RNA with expected changes in total RNA by considering transcript half-life.[28] By analyzing the response of murine fibroblasts to type I and II interferons we found that changes in total RNA can be predicted with high accuracy based on the true transcriptional changes obtained from nascent RNA and transcript half-life (Fig. 3B). Thus, differences between observed and expected changes in total RNA can be used to discriminate changes in RNA transcription and decay. In contrast to serum-starvation[24] neither IFNα nor IFNγ treatment significantly affected RNA decay in murine fibroblasts within the first hour of treatment.[25]

To identify the relative contributions of RNA transcription and decay to changes in total RNA abundance, pre-existing, untagged RNA can also be captured and analyzed.[25] Thereby, changes observed only in one, two or all three of the different RNA fractions can be differentiated and properly interpreted. In addition, the complementarity of the three RNA fractions deriving from a single RNA sample can be used to assess the confidence of the observed changes and identify measurement

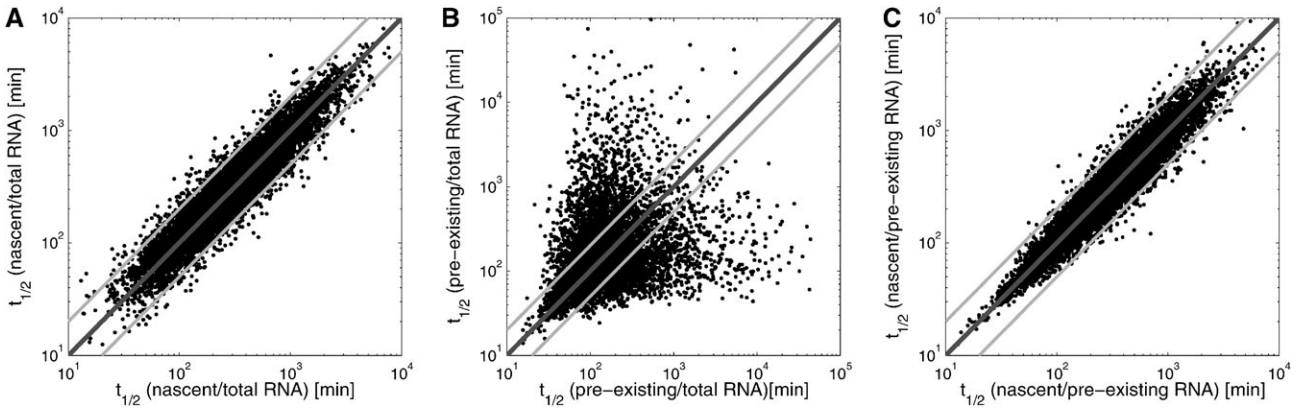

Fig. 4 Precision and reproducibility of transcript half-life determination. Two replicates of nascent, untagged pre-existing and total RNA were simulated. For this purpose, transcript half-lives determined for murine fibroblasts were converted to expected nascent/total RNA (A), pre-existing/total RNA (B) and nascent/pre-existing RNA ratios (C) for a labeling time of 1 h. For each gene and replicate, the observed value was then drawn from a normal distribution with the expected ratio and standard deviation 0.2 × the ratio. From these simulated ratios, half-lives were then calculated. In all panels, light grey lines indicate a 2-fold deviation. Half-lives from nascent/total RNA ratios (A) are precise independent of half-life in contrast to half-lives from pre-existing/total RNA ratios (B) which are highly precise for short half-lives but unreliable for longer ones. By using nascent/pre-existing RNA ratios (C), the advantages of the two approaches can be combined.

errors, *e.g.* changes detectable in only one of the three RNA fractions which are not matched by adequate changes in the other two RNA fractions.

RNA half-life analysis

Apart from its use for gene expression profiling, the identification of transcript half-lives also provides helpful information about the function of a gene. Several studies have shown that the transcript half-life is correlated to gene function and regulation[5,26,27,29,30] and even conserved between species.[26,27] A short transcript half-life is characteristic for regulatory genes, in particular transcription factors, whose expression has to be rapidly regulated. A long transcript half-life, on the other hand, is indicative for genes involved in energy metabolism, translation or protein degradation for which stable RNA concentrations are maintained by slow transcript decay. Furthermore, as transcriptional regulation can only be slow, post-transcriptional regulation is likely predominant. In consequence, transcript half-lives may substantially contribute to the regulation of differential gene expression.

Blocking transcription, *e.g.* using actinomycin D (act-D), and monitoring ongoing RNA decay over time using microarrays commonly serves to measure RNA decay rates at the whole transcriptome level.[5,27,30–35] Unfortunately, transcriptional arrest induces a major stress response in the cell which influences key regulatory mechanisms governing RNA decay and may lead to substantial stabilization of individual transcripts.[36–39] Thus, this approach is inherently cell-invasive and cannot be combined with simultaneous measurements of *de novo* transcription. Assuming that RNA synthesis compensates for RNA decay (steady-state-like conditions) transcript half-lives can be determined in a non-invasive way based on the ratios of nascent to total RNA (Fig. 4A).[25] These half-lives are highly precise and reproducible independent of transcript half-life. In contrast, RNA half-lives determined based on measuring RNA decay rates—either by transcriptional arrest or by capturing untagged RNA after 4sU or 4tU tagging—are only precise for very short-lived transcripts but unreliable for medium- to long-lived transcripts (Fig. 4B). To circumvent this problem, the duration of transcriptional arrest or labeling would have to be extended beyond the medium transcript half-life which is infeasible due to toxic effects on the cells. In order to obtain reliable RNA half-lives based on RNA ratios it is crucial to capture even transcripts with low uridine content. Here, the correlation of uracil numbers in a transcript with log-ratios of nascent/total RNA[19] offers an additional quality control for data. Alternatively, RNA half-lives can be determined by pulse–chase experiments.[17] Here, a short 4tU or 4sU pulse is followed by a prolonged chase upon removal of 4tU/4sU and addition of uridine in excess. While this approach allows the direct analysis of the decay rates of nascent transcripts it provides only imprecise measurements for medium- to long-lived transcripts. Its general applicability remains to be investigated.

Finally, the precision of RNA half-lives determined by nascent/total RNA ratios can be combined with the higher precision for very short-lived transcripts ($t_{1/2} < 30$–60 min) of half-lives from pre-existing/total RNA ratios by calculating transcript half-life from ratios of nascent/pre-existing RNA (Fig. 4C). Although this only requires analysis of nascent and untagged pre-existing RNA, the combined analysis of all three RNA fractions (including also total RNA) provides additional advantages. First, normalization between RNA fractions can be performed by linear regression analysis.[25] This additional normalization is necessary as standard normalization methods assume equal overall intensities for all arrays. Second, it provides access to microarray probe set quality control and allows the identification of the optimal probe sets if multiple probes measure the same transcript—optimized for the individual microarray experiment.[26] Finally, it may allow the evaluation of linearity within the dynamic range of microarray measurements or evaluate the validity of mapping reads obtained by high-throughput sequencing.

Conclusions

Gene expression analyses based on total cellular RNA suffer from low sensitivity for short-term changes, low temporal resolution and a bias for changes in short-lived transcripts. These problems can be solved by biosynthetic tagging of nascent RNA with thiol- or brom-containing nucleosides followed by separation of total cellular RNA into nascent RNA and pre-existing RNA. Thus, both RNA synthesis and decay can be studied with superior sensitivity in a single experimental setting. These new developments will be valuable in widening our current understanding of the regulatory principles governing gene expression and will influence how gene expression profiling studies will be conducted in the future.

Acknowledgements

This work was supported by the German Federal Ministry of Education and Research [NGFNplus 01GS0801 to L.D.] as well as the Friedrich-Baur Stiftung to L.D. We would like to thank Ulrich H. Koszinowski for proof-reading the manuscript.

Notes and references

1 M. G. Guenther, S. S. Levine, L. A. Boyer, R. Jaenisch and R. A. Young, *Cell*, 2007, **130**, 77–88.
2 U. Nagalakshmi, Z. Wang, K. Waern, C. Shou, D. Raha, M. Gerstein and M. Snyder, *Science*, 2008, **320**, 1344–1349.
3 G. Robertson, M. Hirst, M. Bainbridge, M. Bilenky, Y. Zhao, T. Zeng, G. Euskirchen, B. Bernier, R. Varhol, A. Delaney, N. Thiessen, O. L. Griffith, A. He, M. Marra, M. Snyder and S. Jones, *Nat. Methods*, 2007, **4**, 651–657.
4 M. Sultan, M. H. Schulz, H. Richard, A. Magen, A. Klingenhoff, M. Scherf, M. Seifert, T. Borodina, A. Soldatov, D. Parkhomchuk, D. Schmidt, S. O'Keeffe, S. Haas, M. Vingron, H. Lehrach and M. L. Yaspo, *Science*, 2008, **321**, 956–960.
5 E. Yang, E. v. Nimwegen, M. Zavolan, N. Rajewsky, M. Schroeder, M. Magnasco and J. J. Darnell, *Genome Res.*, 2003, **13**, 1863–1872.
6 J. Fan, X. Yang, W. Wang, W. H. Wood 3rd,, K. G. Becker and M. Gorospe, *Proc. Natl. Acad. Sci. U. S. A.*, 2002, **99**, 10611–10616.
7 K. Hirayoshi and J. T. Lis, *Methods Enzymol.*, 1999, **304**, 351–362.
8 J. Garcia-Martinez, A. Aranda and J. E. Perez-Ortin, *Mol. Cell*, 2004, **15**, 303–313.
9 M. Schuhmacher, F. Kohlhuber, M. Holzel, C. Kaiser, H. Burtscher, M. Jarsch, G. W. Bornkamm, G. Laux, A. Polack, U. H. Weidle and D. Eick, *Nucleic Acids Res.*, 2001, **29**, 397–406.
10 L. J. Core, J. J. Waterfall and J. T. Lis, *Science*, 2008, **322**, 1845–1848.
11 M. Ohtsu, M. Kawate, M. Fukuoka, W. Gunji, F. Hanaoka, T. Utsugi, F. Onoda and Y. Murakami, *DNA Res.*, 2008, **15**, 241–251.
12 W. T. Melvin, H. B. Milne, A. A. Slater, H. J. Allen and H. M. Keir, *Eur. J. Biochem.*, 1978, **92**, 373–379.
13 M. Ono and M. Kawakami, *J. Biochem. (Tokyo)*, 1977, **81**, 1247–1252.
14 T. A. Woodford, R. Schlegel and A. B. Pardee, *Anal. Biochem.*, 1988, **171**, 166–172.
15 C. Beadling, K. W. Johnson and K. A. Smith, *Proc. Natl. Acad. Sci. U. S. A.*, 1993, **90**, 2719–2723.
16 K. K. Ussuf, G. Anikumar and P. M. Nair, *Indian J. Biochem. Biophys.*, 1995, **32**, 78–83.
17 M. D. Cleary, C. D. Meiering, E. Jan, R. Guymon and J. C. Boothroyd, *Nat. Biotechnol.*, 2005, **23**, 232–237.
18 G. M. Zeiner, M. D. Cleary, A. E. Fouts, C. D. Meiring, E. S. Mocarski and J. C. Boothroyd, *Methods Mol. Biol.*, 2008, **419**, 135–146.
19 M. R. Miller, K. J. Robinson, M. D. Cleary and C. Q. Doe, *Nat. Methods*, 2009, **6**, 439–441.
20 O. Kitahara, Y. Furukawa, T. Tanaka, C. Kihara, K. Ono, R. Yanagawa, M. E. Nita, T. Takagi, Y. Nakamura and T. Tsunoda, *Cancer Res.*, 2001, **61**, 3544–3549.
21 K. Pike-Overzet, D. de Ridder, T. Schonewille and F. J. Staal, *Methods Mol. Biol.*, 2009, **506**, 403–421.
22 M. Saitou, Y. Yabuta and K. Kurimoto, *Reprod. Biomed. Online*, 2008, **16**, 26–40.
23 K. Schutze, Y. Niyaz, M. Stich and A. Buchstaller, *Methods Cell Biol.*, 2007, **82**, 649–673.
24 M. Kenzelmann, S. Maertens, M. Hergenhahn, S. Kueffer, A. Hotz-Wagenblatt, L. Li, S. Wang, C. Ittrich, T. Lemberger, R. Arribas, S. Jonnakuty, M. C. Hollstein, W. Schmid, N. Gretz, H. J. Grone and G. Schutz, *Proc. Natl. Acad. Sci. U. S. A.*, 2007, **104**, 6164–6169.
25 L. Dölken, Z. Ruzsics, B. Rädle, C. C. Friedel, R. Zimmer, J. Mages, R. Hoffmann, P. Dickinson, T. Forster, P. Ghazal and U. H. Koszinowski, *RNA*, 2008, **14**, 1959–1972.
26 C. C. Friedel, L. Dölken, Z. Ruzsics, U. H. Koszinowski and R. Zimmer, *Nucleic Acids Res.*, 2009, in press.
27 R. Narsai, K. A. Howell, A. H. Millar, N. O'Toole, I. Small and J. Whelan, *Plant Cell*, 2007, **19**, 3418–3436.
28 C. C. Friedel, PhD thesis, Ludwig-Maximilians-Universität München, 2009.
29 Y. Wang, C. L. Liu, J. D. Storey, R. J. Tibshirani, D. Herschlag and P. O. Brown, *Proc. Natl. Acad. Sci. U. S. A.*, 2002, **99**, 5860–5865.
30 R. A. Gutierrez, R. M. Ewing, J. M. Cherry and P. J. Green, *Proc. Natl. Acad. Sci. U. S. A.*, 2002, **99**, 11513–11518.
31 A. F. Andersson, M. Lundgren, S. Eriksson, M. Rosenlund, R. Bernander and P. Nilsson, *Genome Biol.*, 2006, **7**, R99.
32 J. A. Bernstein, A. B. Khodursky, P. H. Lin, S. Lin-Chao and S. N. Cohen, *Proc. Natl. Acad. Sci. U. S. A.*, 2002, **99**, 9697–9702.
33 A. Raghavan, R. L. Ogilvie, C. Reilly, M. L. Abelson, S. Raghavan, J. Vasdewani, M. Krathwohl and P. R. Bohjanen, *Nucleic Acids Res.*, 2002, **30**, 5529–5538.
34 D. W. Selinger, R. M. Saxena, K. J. Cheung, G. M. Church and C. Rosenow, *Genome Res.*, 2003, **13**, 216–223.
35 L. V. Sharova, A. A. Sharov, T. Nedorezov, Y. Piao, N. Shaik and M. S. Ko, *DNA Res.*, 2009, **16**, 45–58.
36 S. N. Bhattacharyya, R. Habermacher, U. Martine, E. I. Closs and W. Filipowicz, *Cell*, 2006, **125**, 1111–1124.
37 C. Blattner, P. Kannouche, M. Litfin, K. Bender, H. J. Rahmsdorf, J. F. Angulo and P. Herrlich, *Mol. Cell. Biol.*, 2000, **20**, 3616–3625.
38 C. M. Brennan and J. A. Steitz, *Cell. Mol. Life Sci.*, 2001, **58**, 266–277.
39 M. Gorospe, X. Wang and N. J. Holbrook, *Mol. Cell. Biol.*, 1998, **18**, 1400–1407.

Nucleic Acids Research Advance Access published June 26, 2009

Nucleic Acids Research, 2009, 1–12
doi:10.1093/nar/gkp542

Conserved principles of mammalian transcriptional regulation revealed by RNA half-life

Caroline C. Friedel[1,*], Lars Dölken[2,*], Zsolt Ruzsics[2], Ulrich H. Koszinowski[2] and Ralf Zimmer[1]

[1]Institute for Informatics, Ludwig-Maximilians-Universität München, Munich 80333 and [2]Max von Pettenkofer-Institute, Ludwig-Maximilians-Universität München, Munich 80337, Germany

Received May 13, 2009; Revised June 8, 2009; Accepted June 9, 2009

ABSTRACT

RNA levels in a cell are regulated by the relative rates of RNA synthesis and decay. We recently developed a new approach for measuring both RNA synthesis and decay in a single experimental setting by biosynthetic labeling of newly transcribed RNA. Here, we show that this provides measurements of RNA half-lives from microarray data with a so far unreached accuracy. Based on such measurements of RNA half-lives for human B-cells and mouse fibroblasts, we identified conserved regulatory principles for a large number of biological processes. We show that different regulatory patterns between functionally similar proteins are characterized by differences in the half-life of the corresponding transcripts and can be identified by measuring RNA half-life. We identify more than 100 protein families which show such differential regulatory patterns in both species. Additionally, we provide strong evidence that the activity of protein complexes consisting of subunits with overall long transcript half-lives can be regulated by transcriptional regulation of individual key subunits with short-lived transcripts. Based on this observation, we predict more than 100 key regulatory subunits for human complexes of which 28% could be confirmed in mice ($P < 10^{-9}$). Therefore, this atlas of transcript half-lives provides new fundamental insights into many cellular processes.

INTRODUCTION

mRNA levels in a cell are determined by the relative rates of RNA synthesis by polymerases and degradation by nucleases. Constant transcript levels reflect an equilibrium of RNA synthesis and decay while changes in transcript levels may be caused by alterations in either of them (1). State-of-the-art gene expression profiling allows precise measurements of total transcript abundance on whole transcriptome level but cannot distinguish whether changes in total mRNA are due to alterations in *de novo* transcription or in decay. RNA decay rates have previously been determined by blocking transcription, e.g. using actinomycin D (act-D), and subsequently monitoring ongoing RNA decay over time (2–8). If RNA decay continues at the same rate after inhibition of transcription, decay rates for thousands of transcripts can be obtained. However, transcriptional arrest induces a major stress response in the cell. This influences key regulatory mechanisms governing RNA decay which leads to substantial stabilization of individual transcripts (9–12).

De novo transcription can be measured in a non-disruptive way by introducing 4-thiouridine (4sU) into newly transcribed RNA utilizing nucleoside salvage pathways (13) followed by thiol-mediated isolation of newly transcribed RNA from total RNA (13–18). By combining this technique with standard microarray techniques, newly transcribed RNA can be directly measured for thousands of genes at the same time (14,15,18). Furthermore, with the integrative approach we developed recently total cellular RNA can be separated into both newly transcribed, labeled RNA and pre-existing, unlabeled RNA with high specificity (14). RNA half-lives can then be determined based on both newly transcribed RNA/total RNA ratios as well as pre-existing RNA/total RNA ratios.

In this article, we demonstrate that half-life measurements based on RNA decay, e.g. after blocking transcription, are inherently imprecise for medium- to long-lived transcripts. In contrast, RNA half-lives determined from newly transcribed/total RNA ratios are precise independent of transcript half-life. In this study, we present the first atlas of RNA half-lives in human B-cells and murine fibroblasts determined with this superior precision.

*To whom correspondence should be addressed. Tel: +49-89-2180-4056; Fax: +49-89-2180-4054; Email: caroline.friedel@bio.ifi.lmu.de
Correspondence may also be addressed to Dr Lars Dölken. Tel: +49-89-5160-5290; Fax: +49-89-5160-5292; Email: doelken@mvp.uni-muenchen.de

The authors wish it to be known that, in their opinion, the first two authors should be regarded as joint First Authors.

This atlas was used to identify patterns in transcript half-life conserved in mammals across species and cell types. A transcriptome-wide comparison between species revealed that transcript half-lives are conserved and specifically correlated to gene function. This enabled us to better characterize the regulation of important genes and identify conserved regulatory principles for a broad range of biological processes.

We show that differences in regulation between functionally similar proteins are reflected in differences in the corresponding transcript half-lives. As a consequence, such differences in transcript half-lives can be used to detect differential regulatory patterns for these genes. Most importantly, we provide strong evidence that the activity of protein complexes consisting of multiple subunits with overall long transcript half-lives can be both fast and efficiently regulated by transcriptional regulation of individual key subunits characterized by very short-lived transcripts. Based on this concept, we could identify more than 100 potential key regulators for protein complexes in human for which at least 28% were confirmed in mice. Accordingly, analysis of RNA half-life provides fundamental new insights into conserved regulatory mechanisms of many biological processes. Therefore, the atlas of transcript half-lives we provide in this study will be valuable for further studies on a large variety of biological processes.

MATERIALS AND METHODS

Sample preparation for microarray experiments

Newly transcribed RNA was labeled in human B-cells (BL41) and murine NIH-3T3 fibroblasts by culturing cells in the presence of 4-thiouridine (4sU) for 1 h. Total cellular RNA was isolated, thiol-specifically biotinylated and separated into labeled, newly transcribed RNA and unlabeled, pre-existing RNA using streptavidin coated magnetic beads as described (14) (see also Supplementary Data for details). In addition, RNA decay rates were obtained for NIH-3T3 cells by blocking RNA synthesis for 1, 2 and 3 h using actinomycin D at a final concentration of 5 μg/ml. Three biological replicates per condition were analyzed using Affymetrix HG U133 Plus 2.0 arrays (human) and MG 430 2.0 arrays (mouse). For murine fibroblasts, an additional three replicates were performed for newly transcribed and total RNA to assess the reproducibility of our approach.

Normalization of microarray data

Microarray data were pre-processed with R and Bioconductor (19,20). A first normalization incorporated background correction, normalization and probe-level summarization by GCRMA. As these standard methods assume equal overall intensities for all arrays, a second normalization step is required to compensate for the different amounts of template mRNA present in newly transcribed RNA, pre-existing RNA and total RNA samples. In previous studies based on blocking transcription (e.g. using actinomycin D) this was either done by using reference genes (8) or by fitting the exponential decay model to time series measurements (5). We performed this normalization based on the combined analysis of total, newly transcribed and unlabeled pre-existing RNA from a single RNA sample (14). Since total RNA (N) is quantitatively separated into labeled, newly transcribed (L) and unlabeled, pre-existing RNA (U), normalized ratios of newly transcribed/total RNA and pre-existing/total RNA should add up to 100% and normalization factors can be obtained by a simple linear regression analysis (see Supplementary Data).

Calculation of RNA half-life

RNA decay has been shown to follow first-order kinetics (21) with

$$\frac{\mathrm{d}U}{\mathrm{d}t} = -\lambda U,$$

where λ is the decay rate for a given transcript. The transcript half-life then is $t_{1/2} = \ln 2/\lambda$. At the beginning of labeling, $U(0) = N(0)$. We assume that total RNA at time t is a multiple or fraction of the original concentration, i.e. $N(t) = \alpha(t)N(0)$ with $\alpha(t)$ a function of time. The RNA half-life of a specific probe set is then calculated as (see Supplementary Data for details)

$$t_{1/2} = -t \ln 2 / \ln\left(\frac{U(t)}{N(t)}\alpha(t)\right) = -t \ln 2 / \ln\left(\alpha(t)\left(1 - \frac{L(t)}{N(t)}\right)\right).$$

where $L(t)/N(t)$ and $U(t)/N(t)$ are the normalized ratios of newly transcribed/total RNA and pre-existing/total RNA. The proportionality factor $\alpha(t)$ can be defined in different ways to model different scenarios: $\alpha(t) = 1$ for the steady state and $\alpha(t) = 2^{t/CCL}$ to model cell growth and division where CCL is the cell-cycle length of the cell. In this study, we used steady-state assumptions as reproducibility between replicates was higher than in the cell division model which amplifies measurement errors for long-lived transcripts (Supplementary Figure S1).

Transcript uracil number

To calculate the number of uracils in the spliced transcript for each gene, cDNA sequences for human and mouse were downloaded from the Ensembl site (release 54, May 2009) (22). The uracil number was then calculated as the number of thymines in the cDNA sequence for each gene. For genes with alternatively spliced transcripts uracil numbers were averaged.

Probe set quality score

As genes may be represented by more than one probe set on the array, we defined a probe set quality score PQS based on the difference between 1 and the sum of normalized pre-existing/total RNA ratios and newly transcribed/total RNA ratios (for details see Supplementary Data):

$$PQS = 1 - \left|1 - \frac{L(t)}{N(t)} - \frac{U(t)}{N(t)}\right|.$$

Gene half-life for a gene g is determined using the probe set with the maximum PQS for gene g.

RNA half-life ratio

Differences in transcript half-life between two genes g_i and g_j were calculated as the *RNA half-life ratio*

$$hlr = \exp\left(\left|\log\left(t_{1/2}(g_i)/t_{1/2}(g_j)\right)\right|\right)$$

where $t_{1/2}(g_i)$ is the RNA half-life for gene g_i.

Functional analysis

To identify functional groups significantly over-represented among short- or long-lived transcripts, we compared the overall distribution of RNA half-lives against the distribution of RNA half-lives for specific functional categories. For this purpose the functional categories of the Gene Ontology (GO) (23) were used and GO annotations were taken from the GO website. Only GO terms were analyzed with at least 10 annotated genes. Significance of differences in the distributions was determined with the Kolmogorov–Smirnov test (K–S test) in R (19). *P*-values were corrected for multiple testing using the method by Benjamini and Yekutieli (24), a more conservative version of the method of Benjamini and Hochberg (25), which controls the false discovery rate (FDR) and does not require the tests to be independent. Correction of *P*-values was performed for all ontologies taken together and statistically significant results were determined at a significance level of 0.001.

Analysis of protein families

Protein family annotations were taken from the Pfam database (26) (downloaded 1 August 2008). In total, we obtained 3170 families for human and 3031 families for mouse. Using orthology mappings from the mouse genome database (MGD) (27), protein family members were mapped between species. After removing redundant families, we obtained a final list of 738 families consisting of at least two members with half-lives in both human and mouse. Average RNA half-life ratios for members of the same family or subunits of the same protein complex (see below) were compared against results for randomized half-lives or families/complexes (10 000 randomizations each). *P*-values were calculated as the fraction of randomizations with lower or equal average half-life ratios than the observed average. Transcripts were defined as fast-decaying (slow-decaying) if the corresponding half-life was among the 20% shortest (longest) half-lives in at least one cell line and the 40% shortest (longest) ones in the other cell line. Functional similarity between members of the same family were calculated using the relevance similarity measure defined by Schlicker *et al.* (28) which determines the similarity between GO annotations of two proteins. For our purposes, similarity was calculated separately for the molecular function and biological process ontologies of the GO.

Analysis of protein complexes

Protein complexes for human and mouse (1185 and 285 protein complexes, respectively) were taken from the CORUM database (29) (downloaded 4 June 2008). Complexes were mapped between species and redundant complexes identical to another complex for either species were eliminated. This resulted in a large set containing 1434 non-redundant but partially overlapping protein complexes on which all analysis for both human and mouse were based.

Protein complex subunits with significantly shorter transcript half-life than the rest of the complex were identified by calculating for each subunit p in each complex C the difference ratio:

$$dr(p,C) = \frac{hlr(p,C-p)}{hlr(C-p,C-p)}.$$

Here, $hlr(p,C-p)$ is the average RNA half-life ratio between subunit p and all the other subunits of C and $hlr(C-p,C-p)$ the average RNA half-life ratio between these other subunits. A subunit p was predicted as a regulatory subunit for a complex C if the following conditions were fulfilled: (i) the average RNA half-life ratio for p to the remaining subunits of C was at least 40% higher than the average half-life ratio between these subunits [$dr(p,C) > 1.4$]. (ii) RNA half-life was shorter than the median half-life in human B-cells and murine fibroblasts (~5 h) and shorter than the median transcript half-life in complex C.

RESULTS

RNA half-life measurements in human B-cells and murine fibroblasts

To investigate RNA turnover rates in mouse and human, we analyzed RNA half-lives in human B-cells (BL41) and murine NIH-3T3 fibroblasts (see 'Materials and Methods' section). The murine measurements have recently been published (14). Human B-cells were chosen to compare the data from murine fibroblasts with a cell line of both a different species and cell type to identify conserved regulatory patterns. RNA half-lives were obtained based on both newly transcribed/total RNA and pre-existing/total RNA ratios (Figure 1A and B, and Supplementary Figure S2). In addition, we performed microarray measurements on total RNA following 1, 2 and 3 h of transcriptional arrest by actinomycin D (act-D) in murine fibroblasts (Supplementary Figure S3) in order to compare our new approach with this standard method used to determine RNA decay rates (2–8). While all three approaches provided highly reproducible data for short-lived transcripts ($t_{1/2} < 1$–2 h) only newly transcribed/total RNA ratios yielded reliable data for medium- to long-lived transcripts. Although reproducibility of half-lives increased with longer act-D treatment, differences between 2 and 3 h act-D treatment were still considerable (Supplementary Figure S3) indicating that transcriptional arrest would have to be prolonged by another several hours to obtain accurate transcript half-lives. By simulating the effect of noise on RNA half-life determination (Supplementary Figure S4), we confirmed that this is not a problem of the individual measurements but an inherent feature of RNA half-life measurements based on monitoring the decay of transcripts.

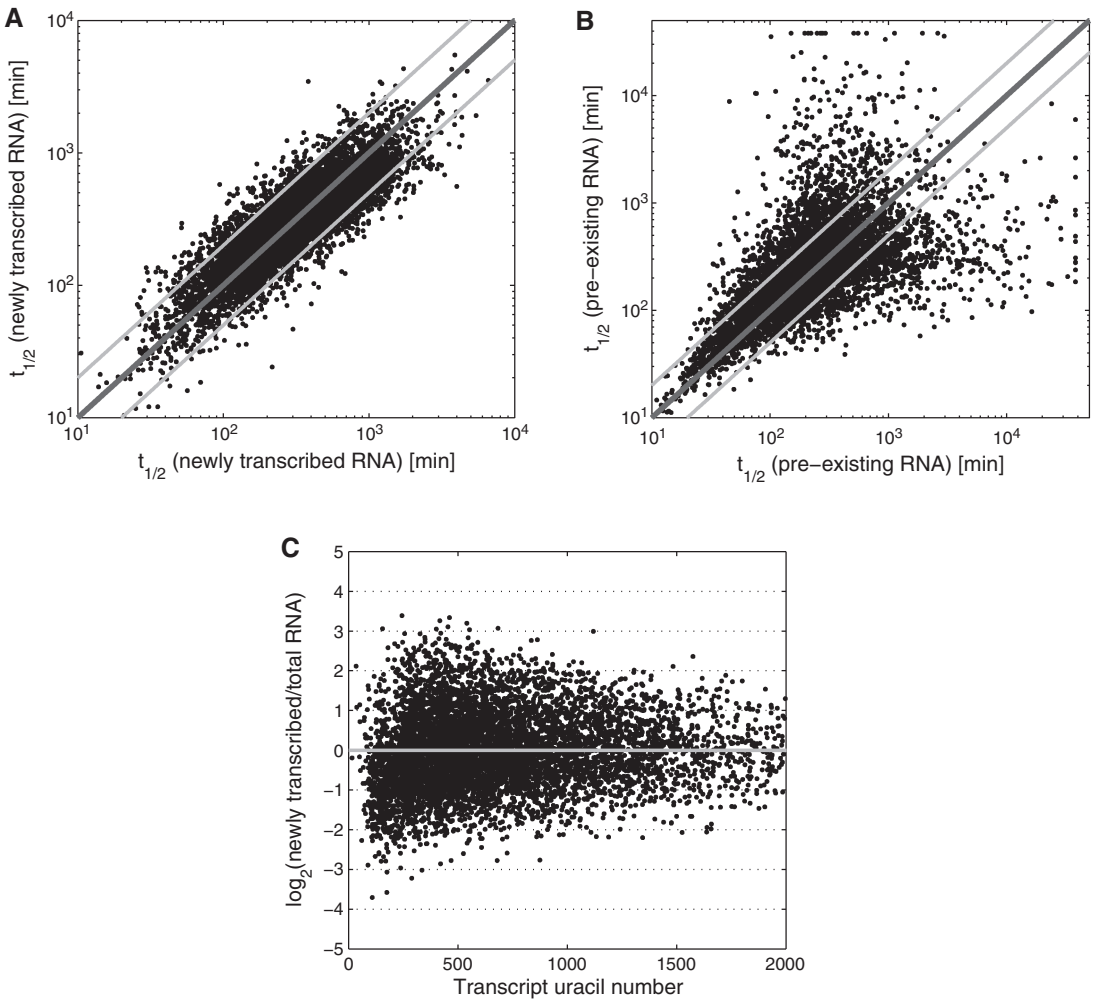

Figure 1. Comparison of RNA half-lives determined in human B-cells based on newly transcribed/total RNA ratios (**A**) and pre-existing/total RNA ratios (**B**) following 1 h of 4sU labeling. RNA half-lives were determined independently for two replicates. The *x*-axis shows the half-life of each gene for the first replicate and the *y*-axis the corresponding half-life for the second replicate. Dark grey diagonals indicate equal RNA half-lives and light grey lines a deviation by a factor of 2. (**C**) Comparison of transcript uracil number (number of uracils in spliced transcript) against the logarithm of newly transcribed/total RNA ratios for human B-cells (correlation coefficient = −0.014). Here, expression levels before the second normalization step were used. The grey line indicates no correlation, i.e. no transcript length bias.

Efficient capture of nascent transcripts is dependent on the incorporation of sufficient amounts of 4sU. This is particularly important for short transcripts with low uracil content. Previously, efficiency of capture of nascent transcripts by the streptavidin-coated magnetic beads was shown to be very high as 80–90% of radioactively labeled nascent RNA could be recovered. Although so far this was not specifically evaluated for short transcripts, reduced capture rates of small transcripts may create a substantial bias when calculating RNA half-lives based on newly transcribed/total RNA ratios (30). To check for this kind of bias, we compared the uracil number for transcripts with the measured ratios of newly transcribed/total RNA for our microarray data. No significant correlation for human B-cells (Figure 1C) and only a weak correlation for murine fibroblasts (Supplementary Figure S2) was observed. Thus, the employed concentrations of 4sU were sufficient for highly efficient capture even of transcripts with low uracil content.

Increasing the accuracy of half-life measurements by using probe set quality scores

Accuracy and reproducibility of half-lives determined from newly transcribed/total RNA ratios can be further increased by assessing probe set quality based on the relationship between newly transcribed, pre-existing and total RNA. On both the Affymetrix MG 430 2.0 arrays (mouse) and the HG U133 Plus 2.0 arrays (human) many genes are represented by multiple probe sets (Supplementary Figure S5). Due to quality differences between probe sets and experimental noise, half-life measurements of different probe sets for a single gene often result in dramatically different results. We solved this problem by calculating a probe set quality score (PQS) for each probe set based on the difference between the sum of measurements for newly transcribed and pre-existing RNA and total RNA levels for each probe set (see 'Materials and Methods' section and Supplementary Data). To evaluate

the performance of this procedure, we determined probe set quality scores independently for each replicate of total, newly transcribed and pre-existing RNA of human B-cells and murine fibroblasts and identified the optimal probe set for each gene for the corresponding replicate. In our study, the same probe sets were independently identified as optimal for the corresponding genes in all three replicates significantly more often than expected by chance (binomial test, FDR corrected $P < 0.05$). In addition, when considering only the optimal probe set for each gene in each replicate, we observed decreased variations between replicates and increased reproducibility of results compared to the standard averaging approach (Supplementary Figure S5). This indicates that our approach can identify individual, incorrect measurements but also distinct quality differences between probe sets in an experimental setting.

Conservation of RNA half-life

For both murine fibroblasts and human B-cells, we determined RNA half-lives for more than 8000 genes based on newly transcribed/total RNA ratios using only the optimal probe set for each gene (Supplementary Tables S1 and S2). Median RNA half-life $t_{1/2m}$ was determined at 315 min (95% confidence interval: 240–382 min) in human B-cells and 274 min in murine fibroblasts (225–323 min) (see 'Materials and Methods' section and Supplementary Data). Although median half-lives differ between the two cell lines, this difference is not significant (*t*-test for unequal variance, $P \sim 0.38$). Furthermore, the distribution of half-lives is similar (Figure 2A) and follows approximately a log-normal distribution in both species. Using orthology tables between human and mouse genes from the MGD (27), transcript half-lives were compared for 4825 genes with RNA half-lives for both species (see Figure 2B). The average half-life ratio (hlr, see 'Materials and Methods' section) between human and mouse was 1.8 and ~67% of genes were within the two-fold range. Although variation between species was significantly larger than between different replicates for the same species and experiment (hlr = 1.2–1.3), it was significantly lower than the variation between different replicates after 1 h Act-D treatment in murine fibroblasts (hlr = 1.97). In addition, differences in transcript half-life between human and mouse were reduced by filtering genes based on the variation between different replicates for the same species. The lower the half-life ratios between

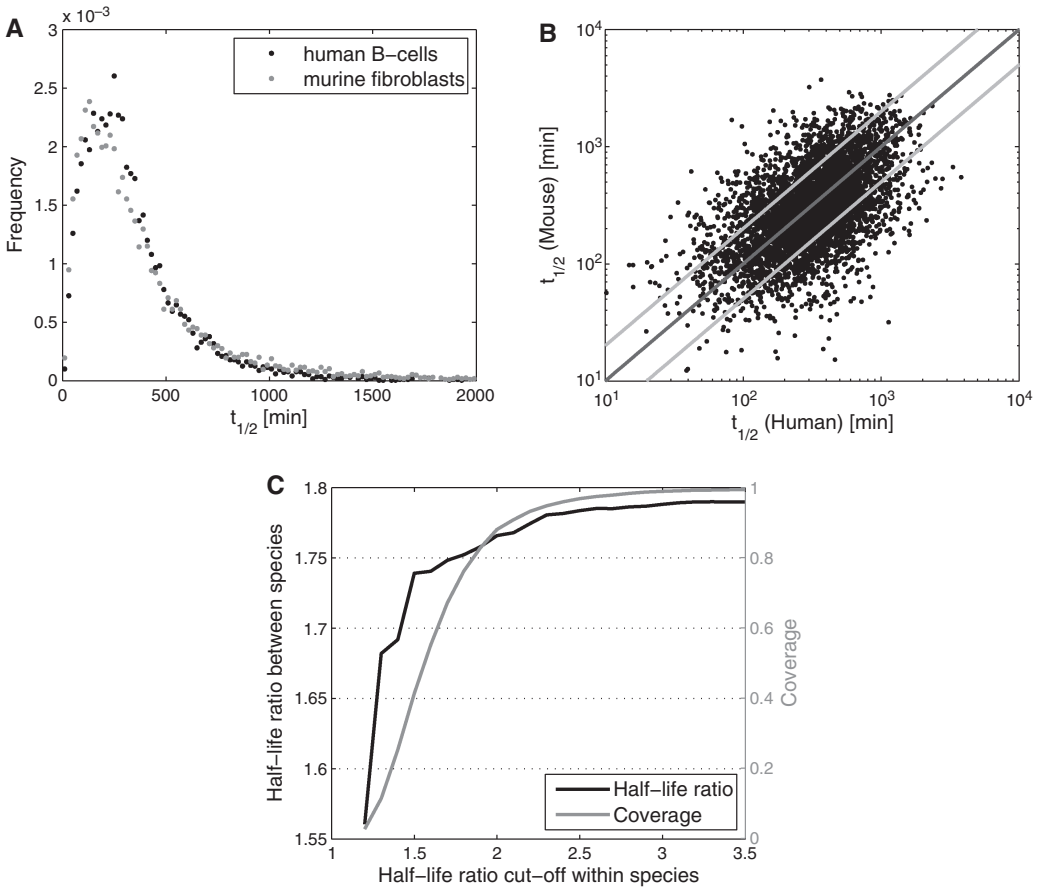

Figure 2. (**A**) Distribution of transcript half-lives for human B-cells and murine fibroblasts. (**B**) Comparison of half-lives between human B-cells and murine fibroblasts for about 5000 genes based on orthology assignments from the MGD database (27). (**C**) Average half-life ratios between species were calculated only for genes for which half-life ratios among different replicates for the same species were below a specific cut-off (*x*-axis). For each cut-off, average half-life ratios between species (black) and coverage (grey), i.e. fraction of genes selected by the cut-off, are shown. Half-life ratios decreased significantly when more selective cut-offs were chosen.

different replicates in one species, the lower were the half-life ratios between the two species (Figure 2C). Furthermore, for only 18 genes (~0.37%) the deviation between species was significant (*t*-test for unequal variance, FDR corrected $P < 0.01$). A list of these genes is provided in Supplementary Table S3.

Association of transcript half-life and gene function

Previous studies of RNA half-lives based on inhibition of transcription have shown that mRNAs of transcriptional genes are preferentially short-lived while transcripts involved in the metabolism of the cell are quite stable (5,8,31). Based on the RNA half-lives determined in this study, we performed a comprehensive analysis of GO terms (for detailed results see Supplementary Table S4 and S5) to associate functional categories with differences in half-life distribution (see 'Materials and Methods' section). In both species, short-lived transcripts were characteristic for genes involved in the regulation of transcription ($P < 10^{-16}$) and signal transduction ($P < 0.007$) (Figure 3A and Supplementary Figure S6). Signal transduction has so far only been associated with fast transcript decay in *Arabidopsis* (5). Interestingly, short half-life was specific only for regulators of transcription and signal transduction as a comparison of the half-life distribution for regulator genes neither involved in transcription nor signal transduction against the distribution for all genes showed no significant difference. Furthermore, previous observations of fast transcript decay for apoptosis and cell cycle transcripts (8) could not be confirmed as no significant difference in the half-life distribution was observed (Supplementary Figure S6).

Significant enrichment for very long RNA half-lives was found for genes involved in cellular respiration and energy metabolism as well as translation and protein decay by the proteasome. Enzymes and protein complexes involved in all parts of energy metabolism consistently had half-lives of more than 5 h both in human and mouse (Supplementary Figure S6 and Table S6). Interestingly, our method revealed a behavior of translational genes not previously described. While the frequency of transcription and signal transduction regulators steadily decreased with increasing RNA half-life (Figure 3A) and the frequency of genes involved in metabolic processes like energy metabolism and the proteasome steadily increased

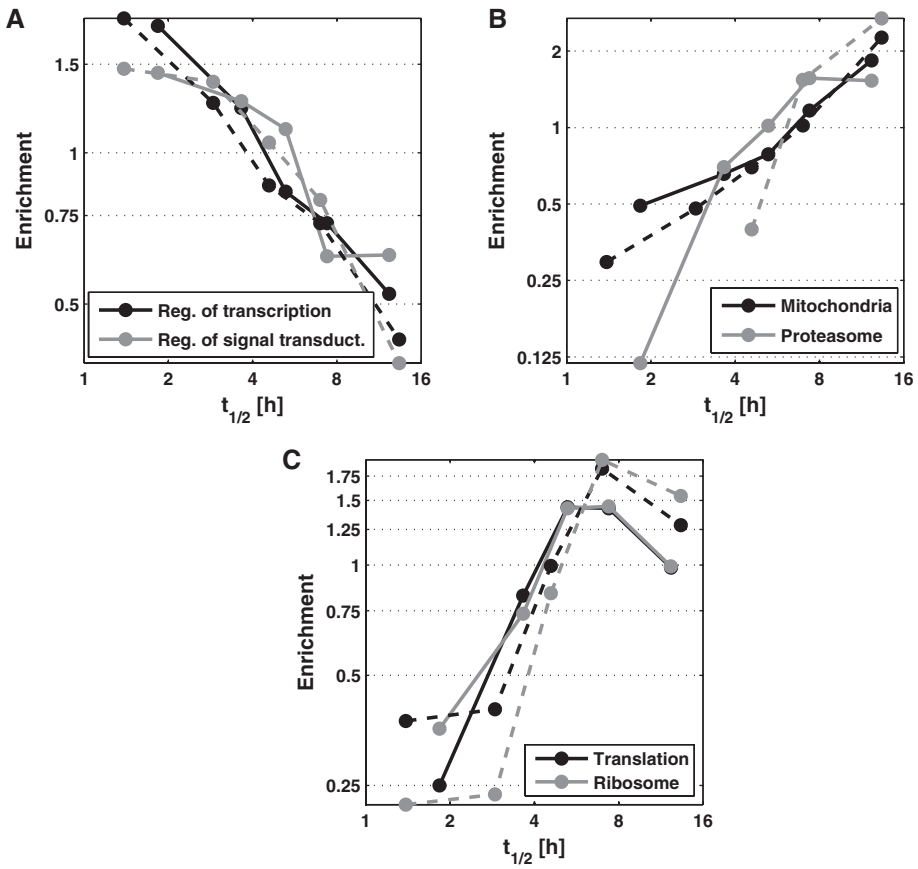

Figure 3. To illustrate the correlation between gene function and transcript half-life, we determined the enrichment of specific functional category (*y*-axis) within different intervals of transcript half-life (*x*-axis) for human B-cells (solid lines) and mouse fibroblasts (dashed lines). For this purpose, the range of transcript half-lives in human B-cells and mouse fibroblasts, respectively, was divided into five intervals each containing approximately the same number of genes. Enrichment for a specific functional category in each interval was then calculated as the ratio of the frequency for this functional category within this interval divided by the overall frequency for this category. Results are shown for (**A**) transcripts involved in regulation of transcription (black) and signal transduction (grey), (**B**) mitochondrial (black) and proteasomal transcripts (grey) and (**C**) translational (black) and ribosomal (grey) transcripts.

(Figure 3B), translational genes, encoding e.g. for ribosomal subunits or translation initiation factors, clustered in the medium-to-long half-life range and showed a lower frequency on either side (Figure 3C).

Regulation of biological processes by transcript half-life

Since protein family members generally have similar functions, we investigated whether this translates to similar transcript half-lives. Indeed, we found that similarity of transcript half-lives was significantly increased in protein families ($P < 10^{-4}$). However, we also identified a large number of protein families with substantial variations in transcript half-life. 111 of 738 protein families (15%) with at least two members for which we obtained half-lives in both human and mouse contained family members with both fast- and slow-decaying transcripts (see 'Materials and Methods' section). A detailed list of these families containing both the genes with the shortest and longest transcript half-life conserved between mice and men is provided in Supplementary Table S7. The median size of these families [22] was significantly larger than for families without such large differences in transcript half-lives (5, Wilcoxon rank sum test $P < 10^{-16}$). The most likely explanation for this finding is that these larger families simply contain more diverse family members with a wider range of functions. Indeed, we found that both similarity of molecular functions and biological processes was significantly lower than for the other families (Wilcoxon rank sum test $P < 0.05$, Supplementary Figure S7). Surprisingly however, we observed that the proteins with the largest difference in half-life did not necessarily show the largest differences in their molecular functions or biological processes. For 44 (39.6%) of the 111 families, functional similarity was actually higher when comparing proteins with short-lived transcripts to proteins with long-lived transcripts than when the other proteins in the family were compared. This indicates that these proteins have a similar function but differential types of regulation. A good example for this finding is the hexokinase gene family. While hexokinase I (HK-I) transcripts decayed slowly ($t_{1/2} \sim 9$ h) as do those of most other genes involved in cellular respiration, transcripts of hexokinase II (HK-II) decayed fast ($t_{1/2} \sim 1$–3.6 h) in both human and mouse. Phosphorylation of glucose by hexokinases is the first step of the glycolysis and hexokinase I is considered a 'housekeeping gene' whose mRNA levels remain stable despite alterations in glucose or insulin levels (32) or feeding conditions (33). Contrary to that, expression of HK-II is induced by a variety of stimuli (32,34–36) thereby accelerating hexose catabolism and regulating blood sugar levels. Fast changes in the expression of HK-II are supported by the fast turnover of HK-II mRNA. In contrast, slow decay of HK-I transcripts prevents any rapid changes in gene expression. Thus, transcript half-lives for these enzymes are specifically adjusted according to their functional role. We noted the same phenomenon for the family of cytosine triphosphate (CTP) synthases. Here, CTP synthase 1 (CTPS) has a short transcript half-life ($t_{1/2} \sim 3$ h) in both mice and men while CTPS 2 has a long transcript half-life ($t_{1/2} > 11$ h). Although CTP synthases are essential enzymes (37), little is known about functional differences and transcriptional regulation. From our results we predict a similar regulatory pattern as for the two hexokinases. One isoform (CTPS) can be rapidly and transiently induced by transcriptional regulation, e.g. during cell cycle, while RNA concentrations of the other isoform (CTPS2) are stable and provide basal enzyme activity levels.

Short- and long-lived transcripts were also observed for the BCL-2 family which contains both pro- and anti-apoptotic proteins (38) (Table 1). Interestingly, long RNA half-lives were only observed for pro-apoptotic family members—although not for all of them. This provides additional evidence that an arrest in transcription following severe stress conditions could lead to a selective decline of the short-lived anti-apoptotic genes but not the pro-apoptotic ones thereby promoting apoptosis (21). Interestingly, the pro-apoptotic BCL-2 family members BAX and BAK, which share a common domain structure and are generally assumed to substitute for each other (39) stand out with respect to their different transcript half-lives (>12 h versus 2–3 h, respectively) in both mice and men. There is evidence that BAX and BAK play non-redundant roles and are regulated in different ways (40–43). Our results support this non-redundant role indicating that it is facilitated by the differences in transcript turnover. This implies that transcriptional regulation is important for BAK-mediated regulation of apoptosis while BAX activity may be preferentially regulated by post-transcriptional means.

These examples show that analysis of transcript half-life can reveal different types of regulation of proteins which otherwise appear to have very similar function.

Table 1. RNA half-lives for genes in the BCL-2 family containing both anti- and pro-apoptotic genes

Gene	Half-life (h) (human)	Half-life (h) (mouse)
Anti-apoptotic		
BCL2	3.80	3.74
BCL2L1	1.96	1.11
BCL2L2	NA	1.75
BCL2A1	3.72	NA
MCL1	1.07	0.70
Pro-apoptotic		
BAX	**38.77**	**12.14**
BAK1	2.13	3.28
BOK	4.64	NA
BID	**10.02**	4.21
BCL2L11	3.99	0.58
BAD	**11.46**	NA
HRK	**5.14**	NA
BBC3	1.47	NA
BIK	4.66	NA
Uncategorized		
BCL2L13	4.09	2.22

Classification into anti- and pro-apoptotic genes was taken from Youle and Strasser (38). Half-lives longer than the median half-life of ~5 h are shown in boldface. NA means that transcript half-life for this gene could not be determined in the corresponding species due to low expression.

Regulation of protein complexes by transcript half-life

For yeast, it has been previously reported that decay rates of transcripts encoding subunits of the same protein complex are similar (31). To investigate this for human and mouse, we analyzed transcript half-lives for the 1434 non-redundant but partially overlapping human and mouse protein complexes taken from the CORUM database (29) (see 'Materials and Methods' section). In both human B-cells and murine fibroblasts, transcripts with long half-lives were significantly over-represented among transcripts encoding subunits of these protein complexes ($P < 0.0003$). As expected, this was particularly prominent for subunits of the large protein complexes involved in energy and protein metabolism (see Supplementary Table S6). In addition, we found that transcript half-lives for subunits of the same protein complex were significantly more similar to each other compared to random expectation (hlr = 1.8–2.0, $P < 10^{-4}$) even if we accounted for the overall high transcript half-life in complexes by randomizing complex memberships instead of half-lives.

Interestingly, despite this relatively high similarity of RNA half-lives in complexes, individual subunits of some complexes deviated substantially in transcript half-life from the remaining subunits. In principle, a single protein may be involved in several different protein complexes which may be regulated in different ways and, thus, may be characterized by different median transcript half-lives. Therefore, for some subunits their deviation in transcript half-life to one complex might be explained by similarity to another. Nevertheless, even when excluding these proteins, we still identified 155 complexes in human and 164 in mouse (out of 698 and 650 complexes, respectively, for which we had half-lives for at least three subunits) which contained protein subunits with a considerably shorter half-life than the remaining subunits (Figure 4, see 'Materials and Methods' section for details). 61 (~37%) of the complexes with deviating subunits were identified in both species which are significantly more than expected by chance (hypergeometric test, $P < 10^{-5}$). Notably, we found that not only these complexes but also their deviating subunits were conserved. In total, we identified 102 and 108 proteins in human and mouse, respectively, which showed significantly shorter half-lives than the other members of the complexes they were part of (Figure 4). A complete list of these proteins and the complexes they are involved in is provided in Supplementary Tables S8 and S9. For 29 (28%) of these proteins identified in human B-cells the significantly shorter RNA half-life in the corresponding complex could be confirmed in murine fibroblasts (hypergeometric test, $P < 10^{-9}$). For an additional 26 (25%) proteins, RNA half-life in the murine fibroblasts was shorter than the median half-life of the complex but the difference was not sufficiently pronounced.

A short transcript half-life allows both fast up- and down-regulation of gene activity on the transcriptional level (see Supplementary Figure S8) (44). Our results suggest that transcriptional regulation of individual key subunits is an evolutionary conserved mechanism to regulate the activity of protein complexes despite overall long RNA half-lives. One example for this type of regulation is the PBAF (Polybromo- and BAF containing complex) chromatin remodeling complex. Here, only the ARID2 (AT rich interactive domain 2) protein is characterized

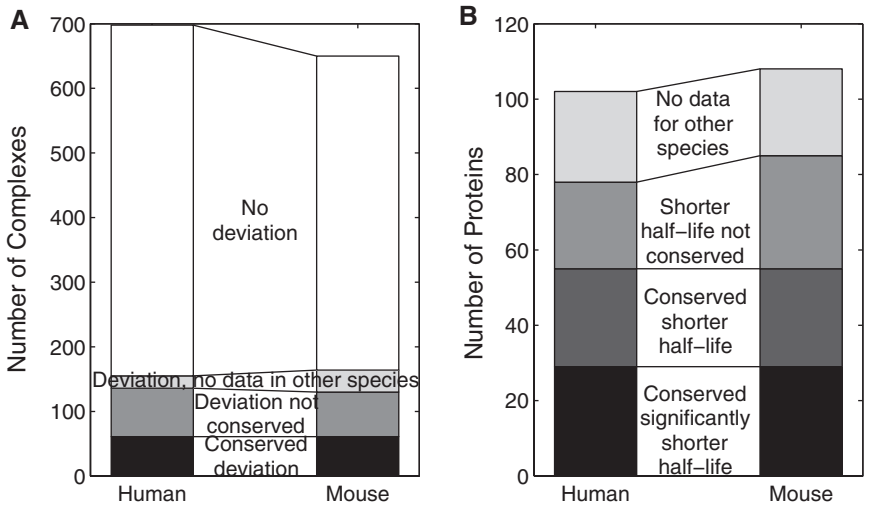

Figure 4. (**A**) Number of complexes containing at least one subunit with (i) significantly shorter transcript half-life than the median RNA half-life in the complex and (ii) no similarity in transcript half-life to any other complex it is contained in (black, grey and light grey) and number of complexes containing no such subunits (white). In the first case, we distinguished between complexes for which the deviation was conserved between species (black), for which it was not conserved (grey) or for which there were no data available in the other species (light grey). Only protein complexes were considered containing at least three subunits for which RNA half-lives could be determined in the respective species. (**B**) Number of proteins with significantly shorter transcript half-life than the remaining subunits in all protein complexes they are contained in. We distinguished between cases in which the significant shorter half-life was conserved (black), a shorter RNA half-life than the median RNA half-life for the complex was observed in the other species although this difference was not sufficiently pronounced (dark grey), the shorter half-life was not conserved (grey) and no data were available for the other species (light grey).

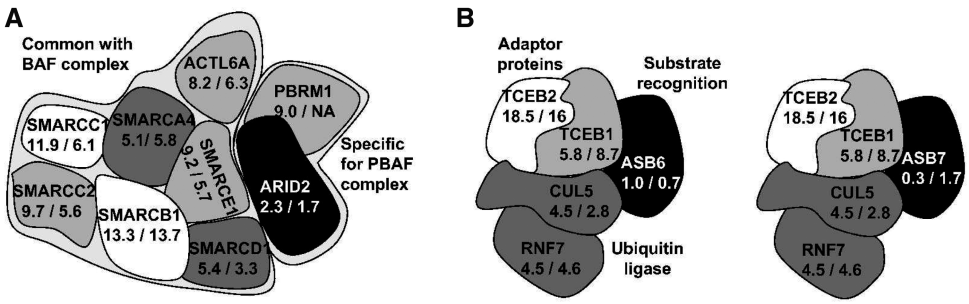

Figure 5. RNA half-lives for the PBAF (**A**) and ubiquitin ligase (**B**) complexes. Half-lives (in hours) for human/mouse are indicated and mapped to grey scales ranging from black (short RNA half-lives) to white (long RNA half-lives). For PBRM1, no transcript half-life could be obtained for murine fibroblasts. For SMARCD1, its RNA half-life in murine fibroblasts was taken from 30 min labeling experiments (14). (A) The PBAF complex consists of several proteins in common with the BAF complex and two specific proteins (ARID2 and PBRM1) (45). ARID2, the only subunit with short transcript half-life in this complex, has been found to be essential for complex stability, potentially by recruiting PBRM1 (45). As most physical interactions in the complex are not characterized, the arrangement of the proteins in this figure does not necessarily represent the true complex structure. (B) Substrate-specificity of the ubiquitin ligase containing CUL5 and RNF7 is determined by binding to different ASB proteins (46,47). TCEB1 and TCEB2 are adaptor proteins which form a heterodimeric complex (Elongin BC) and additionally link the ligase subunits (CUL5 and RNF7) and the ASB protein. Short transcript half-life of the ASB6 and ASB7 subunits allows efficient regulation of complex activity with regard to specific substrates.

by short transcript half-life (Figure 5A). This subunit has previously been shown to be essential for the stability of the PBAF complex (45). Due to its short transcript half-life, the activity of the PBAF complex can be efficiently regulated by transcriptional regulation of the ARID2 protein alone. Another example is the E3 ubiquitin ligase complex (Figure 5B) consisting of CUL5 (Cullin 5) and RNF7 (Ring finger protein 7) linked by the heterodimeric Elongin BC complex (TCEB1 and TCEB2) to an Ankyrin repeat and SOCS box (ASB) protein which serves as substrate-recognition component (46,47). Here, different ASB proteins are responsible for the recognition of different substrates. In our study, we found that two such ASB proteins, ASB6 and ASB7, showed significantly shorter transcript half-lives than the remaining subunits. As these proteins are responsible for substrate recognition, transcriptional regulation of only these subunits suffices to regulate the activity of the complex with regard to specific substrates. As all the other ligase subunits show long transcript half-lives, our results indicate that they are continuously available for binding with various ASB subunits targeting different substrates.

DISCUSSION

Regulation of biological processes occurs at the transcriptional, translational and post-translational level. Optimal control is only achieved by coordinated regulation at all levels. Yet, important information on functional characteristics on many biological processes can already be obtained by analyzing transcriptional regulation. While measurements of differential gene expression indicate which genes are regulated on the transcriptional level in a specific condition, we show in this study that analysis of RNA decay and turnover can provide insights on transcriptional regulation on a more general level.

RNA decay has been studied in a wide range of species: *E. coli* (3), yeast (31), *Arabidopsis* (4,5) and human (8). These studies were based on measurements of RNA decay after transcriptional arrest. In this article, we showed that these RNA half-lives, although quite accurate for short half-lives, are unreliable for medium to long half-lives. Contrary to that, measurements of RNA *de novo* transcription provide reliable and precise results on the whole range of RNA half-lives. Probe set quality scores determined for every probe set based on the combined analysis of newly transcribed, unlabeled pre-existing RNA and total cellular RNA further improved data quality.

One potential bias, which might affect half-life measurements based on newly transcribed RNA, is insufficient capture of short transcripts due to their low number of uracil residues. This would result in underestimation of newly transcribed/total RNA ratios and overestimation of corresponding half-lives. Such a bias was noted in a recent study by Miller *et al.* (30) which used 4-thiouracil (4tU) instead of 4-thiouridine (4sU) which we used in our study. By correlating uracil number of transcripts with newly transcribed/total RNA ratios we demonstrated that 4sU labeling for both human B-cells and murine fibroblasts resulted in sufficient 4sU incorporation to ensure efficient capture of transcript even with rather few (<100) uracil residues. Note that 4sU incorporation into nascent RNAs can be easily enhanced by increasing the applied 4sU concentration in the cell culture medium and, thus, transcript size bias can be experimentally controlled. In contrast, 4tU labeling requires the co-expression of uracil phosphoribosyltransferase (UPRT) of the protozoa Toxoplasma gondii (18). We found 4tU/UPRT based labeling to be strongly dependent on UPRT expression levels as well as the cell type under study but not on the concentration of 4tU (unpublished data). Therefore, labeling efficiency can not be significantly increased by simply adding more 4tU but transcript length bias needs to be controlled for by bioinformatic means (30).

Using our new approach, we determined precise RNA half-lives for more than 8000 genes in both human B-cells and mouse fibroblasts. By choosing two completely

unrelated cell types, we focused on regulatory mechanisms not specific for only individual cell types. For about 5000 orthologous genes, we obtained RNA half-lives in both species and cell types. For the large majority of these orthologous genes, transcript half-lives are conserved across species and cell types. Only 18 out of the 4825 genes compared, i.e. only ~0.37%, actually showed a significant difference in transcript half-life between the two species. Furthermore, variation between species was correlated to the variation observed in the individual experiments for each species. This suggests that to a large degree the observed variations between species were due to variations within the individual experiments and do not constitute important inter-species differences. This does not imply that RNA decay is a static process and that no significant differences in transcript half-life exist in between these two cell lines or species. Our results only show that for conserved genes expressed in both cell lines, transcript half-life is also conserved.

Fast transcript decay allows rapid alterations of steady-state RNA concentrations due to transcriptional changes. At the same time, these changes can also be rapidly reversed. Thus, a short transcript half-life is important for efficient regulation at transcriptional level. Assuming that protein levels and transcript levels are correlated, protein levels of these genes can be efficiently regulated by alteration in transcription rates alone. In contrast, up- or down-regulation of stable transcripts takes a very long time to result in altered total RNA levels which, once established, also persist much longer. Consistent with previous reports, we confirmed a shift towards short half-lives for genes involved in the regulation of transcription and observed this also for regulators of signal transduction. However, a similar shift for genes involved in the regulation of cell cycle or apoptosis as proposed earlier (8) or regulating genes in general (apart from transcriptional and signal transduction regulators) could not be confirmed. Thus, a short transcript half-life is not characteristic for regulators as such but only for regulators of transcription and signal transduction. The most stable transcripts were found for genes encoding for energy metabolism and protein translation and degradation. Interestingly, we observed that RNA half-lives of genes involved in translation cluster in the medium- to long-lived range and decrease in frequency on either side. This indicates that a greater degree of transcriptional control may be required for constituents of the translational machinery than for transcripts coding for proteins involved in protein degradation and energy metabolism. As measurements of RNA decay rates based on transcriptional arrest are inherently imprecise for medium- to long-lived transcripts, it is not surprising that this has been missed by previous studies.

So far, the biological processes and sequence features determining RNA decay are only poorly understood. Previous studies have suggested that certain RNA motifs in untranslated regions (8) or miRNA binding and the presence of introns (5) may play a role. Our approach now allows the analysis of RNA sequence features and motifs which determine fast and slow but also intermediate fast RNA decay. Therefore, the method and data we provide in this study will be valuable for more systematic studies on the mechanisms governing RNA decay.

We identified many biological processes in which closely related members of the same protein family with overlapping function differ significantly in RNA half-life. Here, differences in transcript half-life likely correspond to differences in regulation and, accordingly, functional roles of the corresponding genes. This is best exemplified by hexokinase I and II as well as the pro-apoptotic proteins BAX and BAK. These examples show that transcript half-lives are fine-tuned to support the regulation of cooperative but non-redundant roles of closely related family members. Based on these results, we predict similar regulatory patterns and provide a database for a large number of functionally less characterized genes and processes.

Most proteins function by interacting with other proteins in protein complexes. In this study, we confirmed previous observations in yeast that transcript half-lives for subunits of protein complexes are very similar (31). Furthermore, decay of transcripts for these subunits was found to be generally slow. This implies that most protein complexes are pre-dominantly regulated at the post-translational level. Nevertheless, for more than 150 complexes with overall long transcript half-lives in both human and mouse we identified individual key subunits with a short transcript half-life which deviate significantly from the remaining subunits in all complexes they are part of. For almost a third of these proteins, we found this pattern to be conserved across species. The probability of finding the same complexes and subunits in both species by chance is negligibly small. Therefore, we propose a generalized mechanism employed by cells to facilitate regulation of protein complexes in an efficient and targeted way. For complexes depending on the availability of specific essential components, regulation of complex activity is accomplished by regulating the abundance of only one or few of these key subunits. Thereby, complex activity can be regulated both faster—as most subunits are available and may have already assembled—and more energy efficient than by regulating all complex members. With the two examples of the PBAF complex and the E3 ubiquitin ligase complex, we demonstrated how transcriptional regulation of individual key subunits which are e.g. critical for either complex formation and stability (for the PBAF complex) or specificity (for the E3 ubiquitin ligase complex) can support efficient regulation of complex activity at the transcriptional level. A similar observation was made by de Lichtenberg *et al.* (48) for protein complexes of the yeast cell cycle. As most of these complexes contained both periodically and constitutively expressed subunits, they suggested a 'just-in-time assembly' (instead of 'just-in-time synthesis') in which the timing of the complex assembly is regulated by transcriptional regulation of only some subunits. Our results indicate that this may not be specific for the cell cycle but a general mechanism by which the function of large protein complex is regulated.

Based on this concept, we predict altogether about 100 key regulatory subunits in more than 150 complexes for both human and mouse. This list can be further

extended by 85 and 67 proteins in human and mouse, respectively, which show a significantly shorter RNA half-life in at least one complex but not all complexes they are contained in. In these cases, their short transcript half-life may be explained by the fact that they are part of a complex for which all subunits have to be regulated strongly on the transcriptional level and, accordingly, have short transcript half-lives. Although these subunits were not included in the predictions for key regulatory subunits, they probably also have an important regulative function within the other complexes they are part of. Further studies on the regulatory subunits we predict in this study are required for a better understanding of the regulation of the involved protein complexes and the biological processes they govern.

SUPPLEMENTARY DATA

Supplementary Data are available at NAR Online.

ACKNOWLEDGEMENTS

We would like to thank Bernd Rädle for his excellent technical assistance.

FUNDING

German Federal Ministry of Education and Research (BMBF NGFNplus 01GS0801 to L.D, U.K, C.C.F, R.Z.); the Friedrich-Baur Stiftung (to L.D.). Funding for open access charge: Ludwig-Maximilians-Universität München and BMBF.

Conflict of interest statement. None declared.

REFERENCES

1. Ross,J. (1995) mRNA stability in mammalian cells. *Microbiol. Rev.*, **59**, 423–450.
2. Andersson,A.F., Lundgren,M., Eriksson,S., Rosenlund,M., Bernander,R. and Nilsson,P. (2006) Global analysis of mRNA stability in the archaeon Sulfolobus. *Genome Biol.*, **7**, R99.
3. Bernstein,J.A., Khodursky,A.B., Lin,P.H., Lin-Chao,S. and Cohen,S.N. (2002) Global analysis of mRNA decay and abundance in Escherichia coli at single-gene resolution using two-color fluorescent DNA microarrays. *Proc. Natl Acad. Sci. USA*, **99**, 9697–9702.
4. Gutierrez,R.A., Ewing,R.M., Cherry,J.M. and Green,P.J. (2002) Identification of unstable transcripts in Arabidopsis by cDNA microarray analysis: rapid decay is associated with a group of touch- and specific clock-controlled genes. *Proc. Natl Acad. Sci. USA*, **99**, 11513–11518.
5. Narsai,R., Howell,K.A., Millar,A.H., O'Toole,N., Small,I. and Whelan,J. (2007) Genome-wide analysis of mRNA decay rates and their determinants in Arabidopsis thaliana. *Plant Cell*, **19**, 3418–3436.
6. Raghavan,A., Ogilvie,R.L., Reilly,C., Abelson,M.L., Raghavan,S., Vasdewani,J., Krathwohl,M. and Bohjanen,P.R. (2002) Genome-wide analysis of mRNA decay in resting and activated primary human T lymphocytes. *Nucleic Acids Res.*, **30**, 5529–5538.
7. Selinger,D.W., Saxena,R.M., Cheung,K.J., Church,G.M. and Rosenow,C. (2003) Global RNA half-life analysis in Escherichia coli reveals positional patterns of transcript degradation. *Genome Res.*, **13**, 216–223.
8. Yang,E., Nimwegen,E.v., Zavolan,M., Rajewsky,N., Schroeder,M., Magnasco,M. and Darnell,J.J. (2003) Decay rates of human mRNAs: correlation with functional characteristics and sequence attributes. *Genome Res.*, **13**, 1863–1872.
9. Bhattacharyya,S.N., Habermacher,R., Martine,U., Closs,E.I. and Filipowicz,W. (2006) Relief of microRNA-mediated translational repression in human cells subjected to stress. *Cell*, **125**, 1111–1124.
10. Blattner,C., Kannouche,P., Litfin,M., Bender,K., Rahmsdorf,H.J., Angulo,J.F. and Herrlich,P. (2000) UV-Induced stabilization of c-fos and other short-lived mRNAs. *Mol. Cell Biol.*, **20**, 3616–3625.
11. Brennan,C.M. and Steitz,J.A. (2001) HuR and mRNA stability. *Cell Mol. Life Sci.*, **58**, 266–277.
12. Gorospe,M., Wang,X. and Holbrook,N.J. (1998) p53-dependent elevation of p21Waf1 expression by UV light is mediated through mRNA stabilization and involves a vanadate-sensitive regulatory system. *Mol. Cell Biol.*, **18**, 1400–1407.
13. Melvin,W.T., Milne,H.B., Slater,A.A., Allen,H.J. and Keir,H.M. (1978) Incorporation of 6-thioguanosine and 4-thiouridine into RNA. Application to isolation of newly synthesised RNA by affinity chromatography. *Eur. J. Biochem.*, **92**, 373–379.
14. Dölken,L., Ruzsics,Z., Rädle,B., Friedel,C.C., Zimmer,R., Mages,J., Hoffmann,R., Dickinson,P., Forster,T., Ghazal,P. *et al.* (2008) High-resolution gene expression profiling for simultaneous kinetic parameter analysis of RNA synthesis and decay. *RNA*, **14**, 1959–1972.
15. Kenzelmann,M., Maertens,S., Hergenhahn,M., Kueffer,S., Hotz-Wagenblatt,A., Li,L., Wang,S., Ittrich,C., Lemberger,T., Arribas,R. *et al.* (2007) Microarray analysis of newly synthesized RNA in cells and animals. *Proc. Natl Acad. Sci USA*, **104**, 6164–6169.
16. Ussuf,K.K., Anikumar,G. and Nair,P.M. (1995) Newly synthesised mRNA as a probe for identification of wound responsive genes from potatoes. *Indian J. Biochem. Biophys.*, **32**, 78–83.
17. Woodford,T.A., Schlegel,R. and Pardee,A.B. (1988) Selective isolation of newly synthesized mammalian mRNA after in vivo labeling with 4-thiouridine or 6-thioguanosine. *Anal. Biochem.*, **171**, 166–172.
18. Cleary,M.D., Meiering,C.D., Jan,E., Guymon,R. and Boothroyd,J.C. (2005) Biosynthetic labeling of RNA with uracil phosphoribosyltransferase allows cell-specific microarray analysis of mRNA synthesis and decay. *Nat. Biotechnol.*, **23**, 232–237.
19. R Development Core Team. (2007) R: a language and environment for statistical computing. *R Foundation for Statistical Computing*, Vienna, Austria.
20. Gentleman,R.C., Carey,V.J., Bates,D.M., Bolstad,B., Dettling,M., Dudoit,S., Ellis,B., Gautier,L., Ge,Y., Gentry,J. *et al.* (2004) Bioconductor: open software development for computational biology and bioinformatics. *Genome Biol.*, **5**, R80.
21. Lam,L.T., Pickeral,O.K., Peng,A.C., Rosenwald,A., Hurt,E.M., Giltnane,J.M., Averett,L.M., Zhao,H., Davis,R.E., Sathyamoorthy,M. *et al.* (2001) Genomic-scale measurement of mRNA turnover and the mechanisms of action of the anti-cancer drug flavopiridol. *Genome Biol.*, **2**, RESEARCH0041.
22. Hubbard,T.J., Aken,B.L., Ayling,S., Ballester,B., Beal,K., Bragin,E., Brent,S., Chen,Y., Clapham,P., Clarke,L. *et al.* (2009) Ensembl 2009. *Nucleic Acids Res.*, **37**, D690–D697.
23. Ashburner,M., Ball,C.A., Blake,J.A., Botstein,D., Butler,H., Cherry,J.M., Davis,A.P., Dolinski,K., Dwight,S.S., Eppig,J.T. *et al.* (2000) Gene ontology: tool for the unification of biology. The Gene Ontology Consortium. *Nat. Genet.*, **25**, 25–29.
24. Benjamini,Y. and Yekutieli,D. (2001) The control of the false discovery rate in multiple testing under dependency. *Ann. Stat.*, **29**, 1165–1188.
25. Benjamini,Y. and Hochberg,Y. (1995) Controlling the false discovery rate: a practical and powerful approach to multiple testing. *J. Royal Statist. Soc. B (Methodological)*, **57**, 289–300.
26. Finn,R.D., Tate,J., Mistry,J., Coggill,P.C., Sammut,S.J., Hotz,H.R., Ceric,G., Forslund,K., Eddy,S.R., Sonnhammer,E.L. *et al.* (2008) The Pfam protein families database. *Nucleic Acids Res.*, **36**, D281–D288.
27. Eppig,J.T., Blake,J.A., Bult,C.J., Kadin,J.A. and Richardson,J.E. (2007) The mouse genome database (MGD): new features facilitating a model system. *Nucleic Acids Res.*, **35**, D630–D637.

28. Schlicker,A., Domingues,F.S., Rahnenfuhrer,J. and Lengauer,T. (2006) A new measure for functional similarity of gene products based on Gene Ontology. *BMC Bioinformatics*, **7**, 302.
29. Ruepp,A., Brauner,B., Dunger-Kaltenbach,I., Frishman,G., Montrone,C., Stransky,M., Waegele,B., Schmidt,T., Doudieu,O.N., Stumpflen,V. *et al*. (2008) CORUM: the comprehensive resource of mammalian protein complexes. *Nucleic Acids Res*., **36**, D646–D650.
30. Miller,M.R., Robinson,K.J., Cleary,M.D. and Doe,C.Q. (2009) TU-tagging: cell type–specific RNA isolation from intact complex tissues. *Nat. Methods*, **6**, 439–441.
31. Wang,Y., Liu,C.L., Storey,J.D., Tibshirani,R.J., Herschlag,D. and Brown,P.O. (2002) Precision and functional specificity in mRNA decay. *Proc. Natl Acad. Sci. USA*, **99**, 5860–5865.
32. Printz,R.L., Koch,S., Potter,L.R., O'Doherty,R.M., Tiesinga,J.J., Moritz,S. and Granner,D.K. (1993) Hexokinase II mRNA and gene structure, regulation by insulin, and evolution. *J. Biol. Chem*., **268**, 5209–5219.
33. Soengas,J.L., Polakof,S., Chen,X., Sangiao-Alvarellos,S. and Moon,T.W. (2006) Glucokinase and hexokinase expression and activities in rainbow trout tissues: changes with food deprivation and refeeding. *Am. J. Physiol. Regul. Integr. Comp. Physiol*., **291**, R810–R821.
34. Osawa,H., Printz,R.L., Whitesell,R.R. and Granner,D.K. (1995) Regulation of hexokinase II gene transcription and glucose phosphorylation by catecholamines, cyclic AMP, and insulin. *Diabetes*, **44**, 1426–1432.
35. Jones,J.P. and Dohm,G.L. (1997) Regulation of glucose transporter GLUT-4 and hexokinase II gene transcription by insulin and epinephrine. *Am. J. Physiol*., **273**, E682–E687.
36. Riddle,S.R., Ahmad,A., Ahmad,S., Deeb,S.S., Malkki,M., Schneider,B.K., Allen,C.B. and White,C.W. (2000) Hypoxia induces hexokinase II gene expression in human lung cell line A549. *Am. J. Physiol. Lung Cell Mol. Physiol*., **278**, L407–L416.
37. Stryer,L. (1995) *Biochemistry,* 4th edn. W. H. Freeman & Company, New York, NY.
38. Youle,R.J. and Strasser,A. (2008) The BCL-2 protein family: opposing activities that mediate cell death. *Nat. Rev. Mol. Cell Biol*., **9**, 47–59.
39. Wei,M.C., Zong,W.X., Cheng,E.H., Lindsten,T., Panoutsakopoulou,V., Ross,A.J., Roth,K.A., MacGregor,G.R., Thompson,C.B. and Korsmeyer,S.J. (2001) Proapoptotic BAX and BAK: a requisite gateway to mitochondrial dysfunction and death. *Science*, **292**, 727–730.
40. Panaretakis,T., Pokrovskaja,K., Shoshan,M.C. and Grander,D. (2002) Activation of Bak, Bax, and BH3-only proteins in the apoptotic response to doxorubicin. *J. Biol. Chem*., **277**, 44317–44326.
41. Cartron,P.F., Juin,P., Oliver,L., Martin,S., Meflah,K. and Vallette,F.M. (2003) Nonredundant role of Bax and Bak in Bid-mediated apoptosis. *Mol. Cell Biol*., **23**, 4701–4712.
42. Klee,M. and Pimentel-Muinos,F.X. (2005) Bcl-X(L) specifically activates Bak to induce swelling and restructuring of the endoplasmic reticulum. *J. Cell Biol*., **168**, 723–734.
43. Samraj,A.K., Stroh,C., Fischer,U. and Schulze-Osthoff,K. (2006) The tyrosine kinase Lck is a positive regulator of the mitochondrial apoptosis pathway by controlling Bak expression. *Oncogene*, **25**, 186–197.
44. Alon,U. (2006) *An Introduction to Systems Biology: Design Principles of Biological Circuits*. Chapman and Hall/CRC, Boca Ration, FL.
45. Yan,Z., Cui,K., Murray,D.M., Ling,C., Xue,Y., Gerstein,A., Parsons,R., Zhao,K. and Wang,W. (2005) PBAF chromatin-remodeling complex requires a novel specificity subunit, BAF200, to regulate expression of selective interferon-responsive genes. *Genes Dev*., **19**, 1662–1667.
46. Kohroki,J., Nishiyama,T., Nakamura,T. and Masuho,Y. (2005) ASB proteins interact with Cullin5 and Rbx2 to form E3 ubiquitin ligase complexes. *FEBS Lett*., **579**, 6796–6802.
47. Heuze,M.L., Guibal,F.C., Banks,C.A., Conaway,J.W., Conaway,R.C., Cayre,Y.E., Benecke,A. and Lutz,P.G. (2005) ASB2 is an Elongin BC-interacting protein that can assemble with Cullin 5 and Rbx1 to reconstitute an E3 ubiquitin ligase complex. *J. Biol. Chem*., **280**, 5468–5474.
48. de Lichtenberg,U., Jensen,L.J., Brunak,S. and Bork,P. (2005) Dynamic complex formation during the yeast cell cycle. *Science*, **307**, 724–727.